Title

Sulfur Cathode

ISBN

9781786342492

Authors

Cairns, Elton J

Hwa, Yoon

Publication Date

2017-08-01

DOI

10.1142/9781786342508_0002

Peer reviewed

Chapter 2: Sulfur Cathode

Elton J. Cairns[*†,‡] **and Yoon Hwa***

**Energy Storage Group, Lawrence Berkeley National Laboratory, 1 Cyclotron Road, Berkeley, CA 94720*

† *Chemical and Biomolecular Engineering Department, University of California, Berkeley, CA 94720*

‡ *ejcairns@lbl.gov*

1 Introduction

Since the 1990s, human life has greatly changed because commercial lithium (Li) ion batteries were first released by Sony[1] and became widely used for small electronic devices, which allow people to use their electronics without power cables, i.e., popularization of portable electronics. More recently, the application of Li ion batteries has been expanding to large systems such as electric vehicles (EVs), advanced portable electronics and large scale stationary energy storage systems, because environmental pollution and limited deposits of fossil fuel issues came to the fore, which makes the development of the next generation of energy sources essential. Unfortunately, it is a great challenge for conventional Li ion cells because the performance of Li ion cells hasn't improved as fast as the increase of demand for high-performance portable electronics and is not satisfactory for emerging market demands such as electric automobiles and aircraft. For example, an EV that is fully operated by batter power requires a high specific energy of ~ 350 Wh kg^{-1} at the 3-hour discharge rate with reasonably low cost.[2] The specific energy (Wh kg^{-1}) of a cell is technically determined by the operating voltage (V) and the specific capacity (Ah kg^{-1}) of the cell, however, conventional Li ion cells composed of a carbon anode and a

transition metal oxide cathode can offer only about 100 ~ 200 Wh kg^{-1} of practical specific energy due mainly to low specific capacity of the transition metal oxide cathode (theoretical specific capacity of $LiCoO_2$ cathode:[3] 274 Ah kg^{-1}). Even the theoretical specific energy of conventional Li ion cells (500 ~ 600 Wh kg^{-1}) is not far from the practical requirement for EV applications, so it seems very unlikely that any Li-ion cell can meet the 350 Wh/kg goal. For these reasons, seeking the next generation of rechargeable cells with higher specific energy has become essential.

Even though elemental sulfur was first investigated in the 1960s as a cathode material for light metal (Li, Na) based electrochemical cells,[4, 5] sulfur has recently attracted a great deal of interest and been intensively researched due to its advantages as cathode material for Li rechargeable cells such as a large theoretical specific capacity, low cost, abundance and low environmental impact. The hundreds of research articles and reviews published since 2010 reflect how much the Li/S cell has attracted researchers' interest.[6-20] In the Li/S cell system, the sulfur cathode can accommodate 2 Li ions per S atom by the electrochemical reaction shown below:

$$S_8 + 16Li^+ + 16e^- \leftrightarrow 8Li_2S \quad (E^0 = 2.15 \text{ V vs. } Li/Li^+) \qquad (1)$$

The large theoretical specific capacity (1675 mAh/gS) of the sulfur cathode obtained by reaction (1) can compensate for its relatively low redox potential compared to that of transition metal oxide cathodes, so the Li/S cell can offer a theoretical specific energy of ~ 2600 Wh/kg and a theoretical energy density of 2800 Wh/L under the assumption of complete Li_2S formation during the discharge process, which is much larger than that of the Li ion cell ($LiMO_2$/graphite system: ~ 500 Wh/kg).[21] Besides, sulfur is one of the most plentiful and widespread elements in the world, so it is much less expensive (~$150/ton) than the cobalt and nickel that are employed

as cathode materials for Li ion cells. In addition, the common sulfur cathode has technical similarity to the fabrication of Li ion cell cathodes, therefore, the technological entry barrier for being adapted to practical rechargeable cell manufacture is relatively low. These advantages of the sulfur cathode allow the Li/S cell to be a strong candidate for the next generation rechargeable cell.

Despite the promising advantages, multiple scientific and technical challenges for the sulfur cathode need to be overcome in order to develop a practical Li/S cell; a large volumetric change of about 80 % occurs upon the formation and decomposition of Li_2S during the discharge and charge processes, resulting in mechanical failure of the sulfur cathode;[22, 23] the electronically insulating nature of S and Li_2S limits complete conversion of sulfur to Li_2S. Especially, formation and growth of Li_2S on the surface of the sulfur cathode during discharge impedes further lithiation of sulfur owing to its poor electronic and Li ion diffusivity;[24] and the dissolution of lithium polysulfides (Li_2S_n = 2~8) into most liquid electrolytes leads to both active material loss from the cathode and the shuttle effect, where dissolved lithium polysulfides diffuse to the surface of the lithium metal anode and form an insoluble Li_2S (or Li_2S_2) layer on its surface resulting in low Coulombic efficiency of the cell.[25] By understanding reaction and failure mechanisms of the sulfur cathode, important keys for the design of the sulfur cathode can be deduced: (1) mechanical stability of the sulfur cathode during cycling; (2) improvement of electronic and ionic conductivities of the sulfur cathode; (3) protection in order to suppress the dissolution of lithium polysulfides into the liquid electrolyte; (4) physical or chemical trapping of lithium polysulfides in order to suppress the shuttle effect. These must be addressed for rational design of a sulfur cathode to achieve a high specific energy Li/S cell, and the design of the cathode should not be only aimed at developing sulfur-based active materials, but also should

consider the other components of the electrode such as binder, additives and current collector.

A goal of this chapter is to provide an overview of recent research on the sulfur cathode that represents the notable achievements and to discuss the scientific and technical challenges for developing practical Li/S cells. Various effective approaches and concepts to improve the electrochemical performance of the sulfur cathode with regard to all cathode components including sulfur-based active materials, binder, additives as well as current collectors will be discussed. In particular, remarkable strategies used to improve the cell performance significantly will be highlighted. The additional interlayer commonly placed between the cathode and the separator in the cell will be included in this chapter because of its importance although it is not a part of cathode. Finally, perspectives for further advances toward practical, high specific energy Li-S cells will be provided.

2 Nano-structured Sulfur as Active Material

2.1 Introduction

Since nano-technology has been used in battery engineering, electrode materials can be manipulated and engineered at the nano-scale, which may greatly change the physical and chemical properties. Many kinds of materials have resurfaced and been studied as electrode materials because significantly different electrochemical behaviors of the materials are exhibited when they are nano-sized. In the electrochemical cell, because the Li ion diffusion rate in solid particles is much more sluggish than the rate of Li ion movement in a liquid electrolyte, the

impedance due to Li insertion/extraction can be significantly lowered by reducing the length of the Li ion diffusion pathway through the particles.[26, 27] In particular, this approach can be very effective if the lithiated phase of the host has poor electronic and ionic conductivity. During the electrochemical lithiation process, a new phase first forms at the surface of the particle and grows into the interior part, but poor conductivity of the new phase can impede Li ion insertion, which results in limited utilization of the active material. So the active material can be more fully utilized as the particle size of the active material decreases. In addition, nano-sized particles can have better mechanical stability against fracture during electrochemical cell cycling. Volume change commonly occurs when the host material forms an alloy phase with Li during lithiation and the degree of volume change depends on the crystal structure of the host material and the amount of Li accommodated. But some materials such as silicon, tin and sulfur expand too much compared to the original volume and that causes pulverization of the particles (or electrode). If pulverization of the particles occurs, the fragments (or some part of the electrode laminate) will lose electrical contact with the current collector rendering it no longer available for electrochemical reaction, resulting in capacity degradation. The pulverization problem is a very critical issue for some anode materials for Li ion cells such as silicon and tin. Recent advances show significantly improved electrochemical performance of the cell by using nano-sized particles of active material. It is revealed that nano-sized particles are mechanically more stable than micron-size particles when the volume changes by reaction with Li due to facile strain relaxation.[28-30] As is well known, sulfur and the lithiated solid phase (Li_2S) have very poor conductivity and sulfur particles expand by up to 80 % compared to the original volume of the S particle. So, based on the discussion above, the slow lithiation of sulfur could be addressed in the same manner, so the particle size of sulfur should necessarily be reduced in order to have high

utilization of sulfur and improve the mechanical stability of the electrode.

The electrochemical performance of nano-engineered sulfur can be further improved when it forms unique composite structures with complementary materials such as additional media that can improve physical and chemical properties or provide new advantages to the sulfur cathode. Sulfur/porous material nano-composites is one of the most popular designs because nano pores not only provide the space to accommodate the volume expansion of sulfur during lithiation, but also physically trap polysulfides in its space, which is called the 'polysulfide reservoir' concept. Thus, long cycle life with good Coulombic efficiency of the cell can be achieved with this concept. Porous carbons or metal oxides are commonly employed for porous media. The core-shell nano-structure is another representative design, consisting of a core material (main component) surrounded by a shell material. In general, the shell material acts as a protection layer to prevent the main material from being physically or chemically degraded, or provide a new property. The shell can also prevent direct contact between the core material and the electrolyte to avoid unnecessary side reactions and sulfur loss.[31] This is very effective for the sulfur cathode because polysulfide dissolution into liquid electrolyte is prohibited if the sulfur particle and the liquid electrolyte are physically separated by the shell. So, the core-shell structured nano-composite with sulfur as the core and a second material that has good electrical conductivity, lithium permeability, and mechanical stability as the shell can be considered as a promising approach for enhancing the electrochemical performance of the sulfur cathode.

Due to the structural benefits of nano-composites, most sulfur cathodes that have shown promising cell performance mainly employ sulfur-based nano-composites instead of pure sulfur powder as the active material. Carbonaceous materials such as porous carbon, graphene (oxide) and carbon nanotubes (CNT) have been extensively researched as second media for the sulfur

cathode due to its reasonably good conductivity, lithium permeability, and additional benefits depending on its physical and chemical structure. Polymers that may be flexible or conductive are also strongly considered as second media to improve electrochemical performance of the sulfur cathode. Besides carbonaceous materials and polymers, some inorganic compounds such as oxides and sulfides and metal organic frameworks (MOFs) have been studied as well. These physical mixture concepts could be further improved when combined with chemical surface functionalization that can chemically trap polysulfide species to suppress the polysulfide shuttle effect.

The concepts briefly discussed above have significantly improved the electrochemical performance of the sulfur cathode. In this section, important previous accomplishments will be introduced and discussed in detail, to help trace recent progress on developing sulfur nano-composites as active materials and understand how they work. Organosulfur compounds as cathode material will also be briefly discussed.

2.2 Sulfur/Carbon Nano-composites (~ 12 pages)

Sulfur/carbon nano-composites have been intensively researched for developing advanced sulfur cathodes because most carbonaceous materials have good electronic conductivity so it can compensate for the inadequate electronic conductivity of sulfur (5×10^{-30} S cm^{-1} at 25 ℃) resulting in improvement of sulfur utilization, especially at high rates. Various carbonaceous materials have been investigated in order to improve the electrochemical performance of sulfur cathodes and they can be classified according to their physical structure; (1) nano-porous carbon, (2) one dimensional carbons such as carbon nanotubes (CNT) and carbon nanofibers (CNF) and (3) two dimensional carbons such as graphene and graphene oxide. Basically, carbonaceous

materials have reasonably good electrical conductivity and Li ion transport, so they can provide a stable conductive pathway, which could influence the electrochemical performance of the sulfur cathode positively. Furthermore, those carbonaceous materials offer their own advantages depending on their physical and chemical structure, so various sulfur/carbon nano-composites can be designed.

There are several methods to fabricate sulfur/carbon nano-composites such as the infiltration method, high energy mechanical ball milling, precipitation of sulfur onto carbon surfaces, the hydrothermal method, and wrapping sulfur with two dimensional carbonaceous materials. Unfortunately, the chemical vapor deposition (CVD) method which is one of the most popular and effective methods for synthesizing core-shell nano-structures cannot be used with sulfur due to the low melting temperature of sulfur (~ 115 ^{o}C) that is much lower than the common operating temperature of the CVD process (above 450 ^{o}C depending on the carbon precursor gas). Instead, the infiltration method by heat treatment (commonly conducted at 155 ^{o}C, where the viscosity of liquid sulfur is the lowest) is used to embed sulfur into the inner spaces of carbon particles. A vacuum atmosphere can help to insert sulfur into carbon particles during heat-treatment.

2.2.1 Sulfur/Porous Carbon Nano-composites.

Porous materials are solid media containing pores and voids in their structure and are commonly categorized into microporous (pore size: $\leq$ 2 nm), mesoporous (pore size: 2 $\sim$ 20 nm) and macroporous materials (pore size: $>$ 50 nm) depending on pore size, which was defined by Sing *et al*. in 1985.[32] In addition to these classifications of porous structure, the term ‘nanoporous material’ has been popularly used, which refers to materials with a pore size of $\leq$ 100 nm in

diameter. Porous materials have been intensively studied as a component of sulfur-based composite materials for Li/S cells because the pores in the structure of the materials can play an important role in improving the Li/S cell lifetime by accommodating volume expansion of up to 80 %, so mechanical fracture of the sulfur cathode can be avoided as a result. Furthermore, pores can physically trap lithium polysulfides that are formed by the electrochemical reaction of sulfur with lithium (and can dissolve into liquid organic electrolytes), resulting in better cycle life of the Li/S cells. Among many porous materials, porous carbonaceous materials necessarily attract researchers' attention, due to the diverse methods to prepare a porous structure and a good electrical conductivity in order to improve the electrochemical performance of the Li/S cells. Traditional methods to synthesize porous carbon are categorized by T. Hyeon *et al*. as follows;[33] (1) chemical, physical activation or their combination[34, 35]; (2) catalytic activation of carbon precursors using metal salts or organometallic compounds[36, 37]; (3) carbonization of polymer blends composed of a carbonizable polymer and a pyrolyzable polymer that doesn't leave carbon residue;[38] (4) carbonization of a polymer aerogel synthesized under supercritical drying conditions.[39] In addition to the above-mentioned methods, uniform and ordered porous structures can be obtained by the template synthesis method with an inorganic template that is rigid and designable. Porous carbon with desired pore sizes and shapes can be obtained with the help of template materials. Template inorganic materials are necessarily stable under the process conditions of carbon formation and removable under a condition which is safe for carbon. Zeolites[40] and silica[41] are representative template materials for the fabrication of porous carbons.

In the early 2000s, a few papers reported on sulfur/porous carbon composites fabricated by heat-treatment of a sulfur/porous activated carbon (pore size of 2.5 nm) mixture for the sulfur cathode materials.[42, 43] In the early works, the sulfur/porous carbon cathodes exhibited an initial

specific capacity of about 800 mAh/g that is about a half of its theoretical value, and then the specific capacity rapidly decreased to about 400 mAh/g during the following cycles at 0.1 C discharge-charge.[42, 43] Significant progress on sulfur/porous carbon nano-composite cathodes with high sulfur utilization were reported by Liang *et al*.[44] and Ji *et al*.[45] in 2009. In Liang's work, a hierarchically structured sulfur/carbon nano-composite was prepared with micro- and mesoporous carbon obtained by the post-activation process of mesoporous carbon using KOH. Mesoporous carbon has a uniform mesopore size of about 7.3 nm, and a Brunauer-Emmett-Teller (BET) surface area of 368.5 m^2/g. After the KOH activation, the BET surface area increased to 1566.1 m^2/g and the volume contributed by small pores from the size of 2 to 4 nm increased without morphological change, which indicates that micro- and small mesopores were generated on the walls of mesoporous carbon. The sulfur/micro- and mesoporous carbon nano-composite cathodes exhibited 1584 and 818 mAh/g of initial discharge capacity and exhibited 700 and 220 mAh/g after 50 cycles at the test specific current of 2.5 A/g when the sulfur contents in the sulfur/micro- and mesoporous carbon composite were 11.7 wt.% and 51.5 wt.%, respectively. In this chapter, all specific capacity and applied currents for testing are based on the mass of sulfur unless it is specified otherwise. For comparison, sulfur/microporous carbon and sulfur/mesoporous carbon nano-composite cathodes were also prepared, however, they exhibited a very low initial specific capacity and very poor capacity stability during 50 cycles. It is suggested that the synergetic effect of different sizes of pores occurs, wherein the micropores provide the volume for retaining sulfur species in the cathode and the mesopores provide an efficient Li ion diffusion pathway and thus confer a high ionic conductivity to the cathode.

[Figure 1]

L. F. Nazar and coworkers reported a sulfur/highly ordered mesoporous carbon (CMK-3)

nano-composite that is comprised of sulfur embedded in the conductive mesoporous carbon framework as shown in Figure 1a.[45] CMK-3 was fabricated using a mesoporous silica (SBA-15) template and sucrose as carbon precursor and the sulfur/CMK-3 nano-composite was prepared by following a melt-diffusion method at 155 ^{o}C. The nano-architecture of the sulfur/CMK-3 nano-composite was intended to act as an electronic and ionic conduit to the nano-sized sulfur encapsulated within and provides pores that not only act as the lithium polysulfide reservoir but also enhance mechanical stability by accommodating the volume expansion of sulfur during lithiation. For further improvement, polyethylene glycol (PEG) was linked to the external surface of the composite, which acts as an additional barrier to suppress lithium polysulfide diffusion out of the cathode structure, resulting in improvement of cycle life. As shown in Figure 1b, the sulfur/CMK-3 and sulfur/CMK-3/PEG nano-composite cathodes exhibited a high initial discharge capacity of about 1000 and 1320 mAh/g respectively at a discharge specific current of 168 mA/g. To verify the effect of CMK-3 as a lithium polysulfide reservoir during cycling, the sulfur contents (%) in the sulfur-free electrolyte of the cells employing sulfur/acetylene black composite, sulfur/CMK-3 nano-composite and sulfur/CMK-3/PEG nano-composite as cathode materials and the morphology changes of the cathodes were investigated after 30 cycles. It was demonstrated that the mesoporous structured sulfur/CMK-3 cathode lost only about 25 % of the total active mass of sulfur, while the sulfur/acetylene black cathode lost 96 % of the total active mass of sulfur into the electrolyte after 30 cycles. The sulfur/CMK-3/PEG cathode showed a minimal amount of dissolved sulfur in the electrolyte, which indicates that the PEG-functionalized surface can serve to trap lithium polysulfides by providing a highly hydrophilic surface chemical gradient that preferentially solubilizes them in relation to the electrolyte. The morphology changes of the electrodes after 30 cycles were shown in scanning electron

microscopy (SEM) images, in which the sulfur/acetylene black composite cathode showed significant surface change caused by deposition of insoluble species while the other two cathodes showed very little change. This work is worth highlighting because it presents a high capacity of about 1320 mAh/g with a relatively higher sulfur loading of about 1.1 mg/cm^2 than that of earlier works and a twofold protection concept was proposed in order to enhance the electrochemical performance by combining two different strategies; i.e. porous structure acting as lithium polysulfide reservoir with functional polymer outer layer.

[Figure 2]

Although Liang *et al.*[44] and Ji *et al.*[45] reported great improvement in terms of specific capacity by employing unique nano-structures, long term cycle life was not demonstrated, which is one of the essential properties for practical Li/S cells. Therefore, much more effort has been devoted to improvement of the cycle life of Li/S cells, since reasonably high sulfur utilization was achieved.[46-66] In 2010, Zhang *et al.* reported on sulfur/microporous carbon nano-composites with a narrow pore size distribution (~ 0.7 nm) as cathode material for Li/S cells and it exhibited good rate capability and cycle life.[46] The specific capacity of ~ 890 and 730 mAh/g were obtained at the test specific currents of 200 mA/g and 1200 mA/g, respectively. The specific capacity of the sulfur/microporous carbon nano-composite cathode was almost recovered when the test specific current was decreased back to 200 mA/g, indicating a good rate capability. The cathode also exhibited an excellent capacity retention of about 80 % for 500 cycles with a high Coulombic efficiency at the test specific current of 400 mA/g, as shown in Figure 2a. The excellent electrochemical performance of the sulfur/microporous carbon nano-composite cathode was due to good conductivity of the carbon matrix and the unique structure that is comprised of fine sulfur embedded in the micro-pores of the carbon matrix. As described

in Figure 2b, fine sulfur particles were highly dispersed and well-encapsulated in the micro-pores (~ 0.7 nm) of the carbon matrix, therefore, the embedded sulfur and formed lithium polysulfides were captured by micro-pores during cycling. As a result, active sulfur loss caused by dissolution of lithium polysulfides and its shuttle reaction and formation of a thick Li_2S layer on the cathode surface can be prevented, resulting in good cycle life and excellent Coulombic efficiency. Interestingly, the sulfur/microporous carbon nano-composite cathode showed only one obvious plateau between 1.5 and 2.8 V, whereas the common sulfur cathodes typically show two-plateau behavior during the discharge process. It is suggested that the sulfur that stayed in the micropores is no longer in the S_8 cyclical structure, instead sulfur and carbon are mixed at the atomic level. Consequently, the corresponding Gibbs free energy of the reaction could change, which is reflected in the voltage profile of the sulfur/microporous carbon nano-composite cathode.

According to the above discussion, the properties of porous carbon such as pore size distribution and defect concentration, which mainly depend on the sources of carbon and the synthesis conditions play an important role in determining the amount of sulfur infiltrated into the pores and to improve the electrochemical performance of the Li/S cell. J.-T. Lee *et al*. reported a sulfur/micro- and mesoporous carbon nano-composite obtained by controlling the chlorination temperature during the synthesis process of silicon carbide derived porous carbon (CDC) in order to obtain a different pore size distribution.[56] According to the SEM and BET test results, the chlorination temperature has a very minor impact on the morphology of the particles, the shape, and the size of the isotherm plots, suggesting that all samples have similar porosity. Although the porosity of three samples are similar, small increases in the volume of the sub-nm micropores, small decreases in the volume of 1.3–3.0 nm pores and a small increases in the size of the largest (3–4 nm) mesopores were calculated using a quenched solid DFT model.

Interestingly, Raman spectra of three samples demonstrated that defect concentration decreased as chlorination temperature increases; for instance, CDC-900 ^{o}C has the lowest defect concentration and the highest volume of the smallest pores, and has the highest S content among the CDC-700, 800 and 900 ^{o}C samples. The comparisons of electrochemical cycling performance of the sulfur/CDC-700, 800 and 900 ^{o}C cathodes at the 0.2 C rate showed that the sulfur/CDC-900 ^{o}C cathode exhibited the highest reversible specific capacity of about 600 mAh/g, while the other cathodes exhibited that of about 400 mAh/g for 100 cycles. Although the reasons for the improvement were not completely revealed, some possible reasons were suggested such as faster Li ion diffusion due to the smaller concentration of defects and side reactions caused by chemical residues in the CDC.

As discussed in the introduction to this section, the core-shell nano-structure is a promising strategy to enhance Li/S cell performance. Commonly, core material/carbon shell nano-composites can easily be synthesized using CVD carbon coatings or carbonization of a carbon precursor shell (commonly a polymer) at a heating temperature of between 450 ~ 1000 ^{o}C. However, the low melting point of sulfur does not allow the use of a high temperature method. Instead, core/shell-like nano-structures can be synthesized by inserting sulfur into macropores or the hollow inner space of micro- or mesoporous carbon shells using the sulfur melt-diffusion method,[49-55] G. He *et al*.[49] and N. Jayaprakash *et al*.[52] reported the sulfur/hollow carbon core-shell nanostructured composite for the Li/S cell cathode material. Hollow carbon shells were produced using a silica template, and then sulfur/porous carbon core-shell nanostructured composites were prepared using the melt diffusion method. Sulfur can be diffused into the inner space of carbon through micro- or mesopores of the shell during the melt-diffusion process. With the sulfur/ hollow carbon core-shell nanostructured composite cathode, high

reversible capacity of about 1000 mAh/g at the 0.5 C discharge rate for 100 cycles was achieved.[49, 52] In addition, G. He *et al.*[49] reported comparisons that show the trade-off relationship between shell porosity and capacity retention. The highest initial capacity of 1300 mAh/g was obtained with the sulfur/carbon core-shell nano-composite that has the highest porosity of the shell, presumably owing to the open structure of the shell, but the cycle life of the cell is very poor. In contrast, the lowest initial capacity was obtained with the least porous carbon shell, but it showed the best cycle stability for 100 cycles. The results might indicate that the open structure of the shell helps to supply enough lithium ions to the surface of the sulfur particles, but allows lithium polysulfides to escape from the core-shell structure.

[Figure 3]

Figure 3 shows the advanced design concept of sulfur/porous carbon core-shell structures that employs a nano-porous carbon matrix with micropores in the outer shell, surrounding the inner meso- and macropores.[53, 54, 57] The micropores existing in the outer shell and in the walls between the meso- and macropores prevent migration of the highly soluble lithium polysulfides into the liquid organic electrolyte due to the strong adsorption of the lithium polysulfides. Furthermore, the desolvation of the electrolyte ions in the micropores might be able to suppress the lithium polysulfide dissolution as the solvent concentration is very low or likely to be close to zero in these micropores (Figure 3a).[61] By contrast, highly soluble lithium polysulfides could form near the surface of sulfur/porous carbon nano-composite when porous carbon has irregular pore structure as shown in Figure 3b. Thus, the polysulfide dissolution into the liquid electrolyte and the shuttling effect occur continuously during cycling. D.-S. Jung *et al.*[54] reported a specific capacity of about 540 mAh/g with excellent capacity retention of 77 % with respect to its specific capacity of the fifth cycle after 500 cycles at the 2.4 C test rate, which

indicates the sulfur/hierarchical porous carbon nano-composite is structurally stable during cycling. A sulfur/ordered meso@microporous carbon nano-composite reported by Z. Li *et al.* also showed good capacity retention of up to 81 % with the specific capacity of about 837 mAh/g at 0.5 C after 200 cycles.[57]

In summary, some design strategies of sulfur/porous carbon nanocomposites in order to enhance the electrochemical performance of the sulfur cathode can be successful according to the discussion above; (1) Optimization of pore size distribution and uniform distribution of sulfur in the pore space, (2) Large pore volume in order to increase the amount accommodated sulfur, which is important to achieve high specific energy of a practical Li/S cell. (3) Highly porous carbon that has a closed structure near the outer surface can trap lithium polysulfides more effectively.

2.2.2 Sulfur/Graphene (oxide) Nano-composite

Graphene is one allotrope of carbonaceous material that is two-dimensionally structured with a continuous array of the hexagonal carbon lattice. Graphene is fundamentally a single layer of graphite, however, it offers extraordinary properties, i.e., very high electronic and thermal conductivity, transparency and excellent mechanical stability, which are good features for enhancing the electrochemical performance of the Li/S cell. Graphene can be normally synthesized using the CVD method and epitaxial growth. Unfortunately, mass production of high quality graphene at low cost, and in a reproducible manner with those methods is still a challenge, which limits the practical rechargeable battery application of pure graphene. As an alternative, reduced graphene oxide (rGO), the reduced product of graphene oxide (GO) by thermal, chemical or electrochemical methods has become interesting due to its relatively high

capability of mass production. GO is a compound of carbon, oxygen and hydrogen and is normally produced by exfoliation of graphite that is oxidized using a strong oxidizing agent. GO commonly doesn't have a perfect graphene structure due to the presence of oxygen-containing functional groups such as epoxy and hydroxyl functional groups on the surface. Because of the structural characteristics of GO, rGO also commonly has many pores that are generated at the site occupied by functional groups after the reduction process. Because of the imperfect structure of GO and rGO, they usually have relatively poor properties compared to pure graphene, however, some properties can almost be identical to those of pure graphene depending on the reduction process.

For the design of sulfur/graphene (oxide) nano-composites, graphene (oxide) is employed as deposition site for sulfur to form a thin sulfur layer or small sulfur particles on the surface or wrapping media that forms a nano-structure similar to the core-shell concept.[26, 67-90] J.-Z. Wang *et al*. reported a sulfur/graphene nanosheet (GNS) composite produced by the melt-diffusion method to form a sulfur layer on the surface of GNS.[73] The initial discharge capacity of pure sulfur and the sulfur/GNS composite cathodes of about 1100 and 1611 mAh/g, respectively, at a test specific current of 50mA/g were demonstrated and the sulfur/GNS composite cathode showed a discharge capacity of about 580 mAh/g after 40 cycles while the pure sulfur cathode showed only about 200 mAh/g. The electrochemical impedance spectroscopy results indicated that the charge-transfer resistance of the cell employing sulfur/GNS composite cathode was lower than that of the cell with pure sulfur cathode, which presumably is able to explain the improvement of the reversible capacity of the cell. Despite the improvement in terms of specific capacity, the capacity retention of the sulfur/CNS composite cathode was only about 36 % after 40 cycles, even with very low sulfur content of about 22 wt.% in the sulfur/CNS composite,

which is not comparable with conventional Li ion cells. The poor cycle life of the sulfur/CNS composite cathode might be due to direct contact of sulfur with liquid organic electrolyte and a lack of a physical or chemical barrier against polysulfide dissolution. This result emphasizes that a simple mixture of sulfur and graphene cannot offer long cycle life, therefore, the sulfur/graphene nano-composite needs to employ an additional strategy to maintain its enhanced specific capacity.

[Figure 4]

A graphene (oxide)-wrapped sulfur nano-composite is one of the unique nanostructures that is intended to physically trap the sulfur and lithium polysulfides by surrounding sulfur particles with graphene (oxide) sheets.[68-71, 81] H. Wang *et al*. reported GO-wrapped sub-micron sulfur particles including carbon black in the structure to improve the conductivity of the cathode. [68] Triton X-100 which is a surfactant containing a polyethylene glycol (PEG) chain was used as a capping agent for sulfur particles to limit the size of sulfur particles in the nanoscale during the synthesis. The strategies of the GO wrapped sulfur nano-composite in order to improve the cell performance are: (1) the outer GO layer on the sulfur nano-particles not only can help to trap the lithium polysulfides as they form, but also provide a flexible cushion to accommodate the volumetric strain caused by volume expansion of sulfur particles during lithiation process, (2) PEG containing surfactant coating provides additional chemical barrier against lithium polysulfides dissolution into liquid electrolyte, (3) the GO and the carbon black improve the electronic conductivity of the sulfur based cathode. The sulfur/PEG, the sulfur/GO without PEG and the sulfur/GO with PEG cathodes were prepared for comparison and they exhibited similar initial specific capacity of 700 ~ 800 mAh/g at the 0.2 C discharge rate. However, the sulfur/GO cathode with PEG only showed a stable cycle life for 100 cycles, while

the other two cathodes showed very poor cycle life. The sulfur/GO cathode with PEG still delivered a specific capacity of about 500 mAh/g after 100 cycles, but the specific capacity of the other two cathodes dramatically decreased to about 300 mAh/g after only 50 cycles, which indicates that sulfur was more effectively retained in the cathode when two types of protection were combined. On the other hand, S. Evers and L. F. Nazar used rGO as both an electrical conduit for insulating sulfur and as a barrier to retard polysulfide dissolution.[69] This work is highlighted by the high sulfur content of about 78 % in the sulfur cathode achieved by excluding conductive carbon additives (rGO used as wrapping media was the only carbonaceous material in the cathode), which is suitable for practical level of sulfur content. The rGO wrapped sulfur cathode achieved a specific capacity of about 700 and 500 mAh/g at the first and 50th cycle, respectively. The results suggest that rationally engineered sulfur/graphene (oxide) nano-composites can provide an opportunity for increasing the sulfur content in the cathode by decreasing the content of conductive carbon additives in order to achieve a high specific energy and energy density of a practical Li/S cell.

A unique core-shell nano-structure that is comprised of hollow graphene nanoshells (HGNs) and inserted sulfur was reported by H.-J. Peng *et al.*,[71] which delivers an extended lifetime of 1000 cycles at 1.0 C with a slow specific capacity decay rate of 0.06 % per cycle (Figure 4(a)). The initial specific capacity of the sulfur/HGNs cathode was up to 1100 mAh/g and it still showed 420 mAh/g after 1000 cycles. The rate capability test results of the sulfur/HGNs cathode showed high discharge capacities of 1520, 1058, and 737 mAh/g at 0.1, 2.0, and 5.0 C, respectively, and then the specific capacity recovered quickly to 1200 mAh/g when the C-rate was decreased to 0.1 C, which indicates the excellent rate capability of the sulfur/HGNs cathode. The excellent electrochemical performance of the sulfur/HGNs cathode

was due to the 3D graphene framework that provides: (1) free space provided by the hollow structure of the graphene nanoshells for accommodating volume expansion of sulfur particles during discharge, (2) a physical protection layer that suppresses lithium polysulfide dissolution into the liquid electrolyte during cycling and (3) stable electron pathways that improve the electronic conductivity of the cathode.

[Figure 5]

In 2011, a notable discovery was reported by L. Ji *et al.*, which demonstrated that the functional groups on the surface of GO have strong adsorbing ability to anchor S atoms and to effectively prevent the subsequently formed lithium polysulfides from dissolving into the electrolyte during cycling.[67] Figure 5(a) shows the carbon K-edge absorption spectra for both GO and sulfur/GO nano-composites, which revealed that the oxygen containing functional groups on GO can enhance the binding of S to the C atoms. The sulfur/GO nano-composite was prepared by the chemical deposition of sulfur onto graphene oxide in a micro emulsion system followed by heat-treatment in order to remove some bulk sulfur. This unique nano-structured sulfur/GO nano-composite cathode showed a very high initial specific capacity of about 1320 mAh/g at 0.02 C and a reversible specific capacity of about 950 mAh/g at 0.1 C for 50 cycles as shown in Figure 5(b). The excellent electrochemical performance of the sulfur/GO nano-composite cathode is due to; (1) improvement of conductivity by the GO in the heat-treated composites, (2) The oxygen containing functional groups on the GO surface immobilize sulfur and lithium polysulfides, (3) very thin and conformal sulfur coating layer shorten the conduction pathway through sulfur and (4) the GO network accommodates the volume expansion caused by the lithiation process of sulfur. A further study on the electronic structure and chemical bonding between sulfur and GO was conducted by L. Zhang *et al*. using X-ray spectroscopies such as X-

ray photoelectron spectroscopy (XPS), near-edge X-ray absorption fine structure (NEXAFS) and X-ray emission spectroscopy (XES).[76] The results revealed that; (1) the incorporation of sulfur can partially reduce the GO and thus improve the conductivity of the GO; (2) the mild interaction between GO and sulfur can not only preserve the fundamental electronic properties of GO but also stabilize the sulfur by direct bonding with the GO sheet, which may prevent the diffusion of Li polysulfides formed during the discharge–charge cycling into the electrolyte. B. Wang *et al.* conducted a theoretical study of the effect of oxygen-containing functional groups to stabilize the polysulfides through molecular dynamic simulations and density functional theory calculations.[91] The results suggested that oxygen-containing functional groups, especially oxygen bonded to vacancies and edges, may be used to stabilize the polysulfides, which can explain the experimentally observed improved cycling stability when graphene-based materials are introduced in the cathode material.

[Figure 6]

In order to reinforce the chemical barrier against lithium polysulfide dissolution or to provide a new opportunity for trapping sulfur and lithium polysulfides, additional functionalities were provided to the surface of graphene (oxide) using various methods such as nitrogen doping,[81, 82] hydroxylation,[80] employing cationic surfactants[88] and so on.[74, 85, 89, 90] Nitrogen doping on the surface of carbonaceous materials is a promising method to enhance electronic conductivity because nitrogen atoms substituting for carbon atoms in the graphite matrix are electron donors and promote n-type conductivity.[92] It is also beneficial for the Li/S cells because nitrogen-containing functional groups on the surface of the carbonaceous materials can trap lithium polysulfides, resulting in improvement of the cycle life of the Li/S cells. For these reasons, various nitrogen-doped carbonaceous materials such as porous carbon,[60, 63] graphene

(oxide)[81, 82] and carbon nanotubes (or fibers)[93, 94] have been employed in the sulfur cathode in order to enhance the electrochemical performance of Li/S cells. Y. Qui *et al*. demonstrated an ultralong cycle life exceeding 2000 cycles at the 2.0 C rate and an extremely low capacity-decay rate (0.028% per cycle) using nitrogen-doped rGO (NG) produced by a thermal nitridation process of graphene oxide in a NH_3 atmosphere at 750 °C as wrapping media on the surface of sulfur nano-particles.[81] Three types of nitrogen functional group such as pyridinic N, pyrrolic N, and graphitic N on NG were demonstrated by N 1s XPS and especially, the first two types are dominant in the product, which are believed to be more effective in alleviating dissolution of lithium polysulfides into the liquid electrolyte and improving their re-deposition process during cycling.[95, 96] The sulfur/NG cathode that is comprised of sulfur (60 %) without any additional carbon additive delivered reversible specific capacities of about 730 and 492 mAh/g at the 100^{th} and 1000^{th} cycle, respectively, and showed a capacity retention of about 44 % after 2000 cycles. The excellent performance of the sulfur/NG cathode was attributed to the NG which not only provides an efficient electrical pathway, but also acts as a sulfur immobilizer using the nitrogen-containing functional groups on the surface of NG. The cetyltrimethyl ammonium bromide (CTAB)-modified sulfur/GO nano-composite cathode reported by E. J. Cairns and co-workers, shows an ultralong service life exceeding 1500 cycles at the 1.0 C discharge rate (extremely low decay rate of 0.039% per cycle) with excellent specific capacity of about 846 mAh/g at 0.05C after 1000 cycles at 1.0 C and about 740 mAh/g at 0.02 C after 1500 cycles at 1.0 C as shown in Figure 6.[88] The excellent electrochemical performance of CTAB-modified sulfur/GO nanocomposite cathode was achieved by a multifaceted approach: (1) graphene oxide acts as a sulfur immobilizer, (2) CTAB-modified sulfur anchored on the functional groups of GO, (3) elastomeric SBR/CMC binder and (4) an ionic liquid-based novel electrolyte containing $LiNO_3$

additive.

Most synthesis methods of sulfur/graphene (oxide) nano-composites discussed above use graphene (oxide) as a sulfur deposition site or wrapping medium on sulfur particles, therefore, the properties of graphene (oxide) such as number of layers and surface area strongly influence the nano-structure of the sulfur/graphene (oxide) composite, which means that the preparation process of graphene (oxide) needs to be conducted with care. Facile synthesis methods for sulfur/graphene (oxide) were developed by J. Xu *et al.*[83] and T. Lin *et al.*[78] using high energy mechanical ball milling (HEMM). The HEMM method is very attractive for practical applications because it allows a scalable one-step synthesis and commonly doesn't require harmful chemicals, so it is feasible for mass production without severe impact on the environment. The "sandwich-like" layered meso-/macroporous sulfur/graphene nanoplatelets (GnPs) were prepared by HEMM with the sulfur-GnP ratio of 7 : 3 (0.7S-0.3GnP, the final sulfur content in 0.7S-0.3GnP was about 65.5 %), indicating that the presence of sulfur in the ball-milled graphite facilitated the formation of 3D nanostructured carbon foams, presumably due to the strong S-S interaction between the edges of the functionalized S-GnP.[83] The 0.7S-0.3GnP cathode showed excellent high C-rate performance with average discharge capacities of 1043.1, 885.6, 756.8, 610.4, 404.8, and 186.5 mAh/g at 0.2, 0.5, 1.0, 2.0, 5.0 and 10.0 C, respectively. Long cycle life of the 0.7S-0.3GnP cathode was demonstrated with a discharge specific capacity retention of about 50 % (966 mAh/g at the first cycle and 485 mAh/g at 500^{th} cycle) after 500 cycles at 2.0 C, which is due to the "sandwich-like" layered meso-/macroporous nano-structure of S-GnP. The electrochemical performance of the S-GnP cathode was further improved by employing additional carbon paper (CP) between the separator and the cathode in order to suppress the lithium polysulfide shuttle to the anode. This is called the 'Interlayer concept' and

will be discussed in separate section. The 0.7S-0.3GnP-CP cell delivered an initial discharge capacity of 970.9 mAh/g and 679.7 mAh/g at the 500th cycle at the 2.0 C rate.

In summation, graphene (oxide) has significant advantages as a component of the sulfur cathode, such as a high electrical conductivity, the immobilizing effect on sulfur and lithium polysulfides depending on its functional groups on the surface, mechanical flexibility as well as a large surface area. It is commonly used as sulfur deposition surface or wrapping media for sulfur nano-particles and it compensates for the low electronic conductivity of sulfur, and physically or chemically suppresses lithium polysulfide dissolution into liquid electrolytes. However, the effectiveness of graphene (oxide) for enhancing the electrochemical performance of the Li/S cell strongly depends on its physical and chemical structure such as defect concentration and degree of oxidation, so it should be engineered very carefully in order to achieve the most promising and reliable performance of the Li/S cell.

2.2.3 Sulfur/1-D Structured Carbon Nano-composites

One-dimensionally (1-D) structured carbonaceous materials such as carbon nanofibers (CNFs) and carbon nanotubes (CNTs) have been employed in many technologies due to their extraordinary thermal and electrical conductivity and mechanical properties. CNT is regarded as a carbon nano-fiber with stacking of rolled graphene layers at specific rolling angles, thus, it forms into perfect cylinders, consisting of a cylindrical wall with a hollow inner space. The properties of CNTs strongly depend on the radius, the rolling angle, and especially, the number of rolled graphene layers which categorize the CNTs into single-walled carbon nanotubes (SWCNTs) and multi-walled carbon nanotubes (MWCNTs). For the Li/S cell application, 1-D structured carbonaceous materials can be employed in the cathode as a conductive additive or a

component of a composite active material, because it can provide a continuous and efficient electrical pathway, thus the reaction kinetics of the sulfur cathode can be enhanced, resulting in an improvement of Li/S cell performance. In the early work conducted by S.-C. Han *et al*., MWCNTs were employed as a conductive additive in the sulfur cathode to improve the electrical conductivity.[97] Two different sulfur cathodes were prepared, with and without MWCNT addition, respectively and were electrochemically tested for comparison. It was demonstrated by cyclic voltammetry (CV) and electrochemical impedance spectroscopic (EIS) techniques that the charge and discharge overpotentials were reduced when the MWCNTs were employed. In addition, the sulfur cathode with the MWCNT additive showed an initial capacity of about 500 mAh/g while that of the sulfur cathode without the MWCNT additive yielded about 400 mAh/g, which verified the effect of the MWCNT as a conductive additive. However, the specific capacity and cycle life of the Li/S cell employing the sulfur cathode with the MWCNT additive were still poor due to the large particle size of the sulfur powder (~ 80 μm) and no protection against lithium polysulfide dissolution into the electrolyte.

L. Yuan *et al*. fabricated a sulfur-coated multi-walled carbon nanotube (sulfur/MWCNT) composite cathode using the melt-diffusion method.[98] The MWCNTs were used as a component of the composite that provides a large surface area to encourage the formation of a very thin sulfur layer, so the sulfur-coated MWCNT composite can have benefits in terms of electrical conductivity by providing a continuous electrical pathway through the 1-D structured MWCNT network, reducing the length of the Li ion diffusion pathway through insulating sulfur. As a result of the composite material preparation, the 1-D structured sulfur-coated MWCNT composite had an average thickness range of sulfur from several to tens of nanometers, depending on the sulfur content in the composite. To verify the benefits of the nano-structure, a sulfur-coated carbon

black cathode and a MWCNT mixed sulfur cathode were prepared for comparison. The results of the electrochemical cycling test at a specific current of 100 mA/g showed that the sulfur-coated MWCNT composite cathode maintained a reversible capacity of about 670 mAh/g after 60 cycles, whereas the other two cathodes exhibited reversible capacities of only about 270 mAh/g after 40 cycles, which confirmed the effect of the nano-structure that improved the electrochemical performance. SEM examination of the cycled cathodes showed a significant difference between the sulfur-coated MWCNT composite cathode and the other two cathodes. In the SEM images, the sulfur-coated MWCNT composite maintained a uniform distribution of sulfur on the cathode whereas the other two cathodes showed obvious aggregation of sulfur (or lithium sulfide) after cycling. Based on the results, it was suggested that the nano-structure of the sulfur-coated MWCNT composite not only helped to enhance the reaction kinetics, but also to stabilize the structure of the sulfur cathode during cycling, resulting in enhancement of the Li/S cell's performance.

[Figure 7]

Although the sulfur-coated CNT nano-composite cathodes improved the electrochemical properties of the Li/S cells, no effective protection barriers against lithium polysulfide dissolution into the liquid organic electrolyte and its shuttle effect were available, thus the specific capacity continuously decreased during cycling. To overcome the lack of protection, a porous material concept discussed above was adopted in order to physically trap lithium polysulfides during cycling.[63, 99-104] L. Ji *et al*. prepared a porous carbon nanofiber-sulfur composite, comprising embedded sulfur in the pores of CNF generated by elimination of poly (methyl methacrylate) during the carbonization of poly acrylonitrile (PAN) wires.[99] The large surface area of the pores in the CNFs was filled with deposited sulfur *via* a solution-based

chemical reaction, and that was confirmed by electron microscopy and BET analysis. Because sulfur was dispersed well in the pores on the highly electronically conductive CNFs, a high initial specific capacity of nearly 1400 mAh/g at 0.05 C could be delivered with ~ 85 % capacity retention after 30 cycles. In addition, the specific capacity of 987 mAh/g was obtained at the 0.2 C after 30 cycles at various C rates, indicating good rate capability of the Li/S cells. S. Xin et al. prepared CNT@mesoporous carbon (MPC) by coating a porous layer on the surface of MWCNT using D-glucose and sodium dodecyl sulfate (SDS) as carbon precursors followed by a carbonization process.[102] Sulfur was inserted into the pores of the outer porous carbon layer using the melt diffusion method to form a coaxial nano-structure consisting of a CNT core and MPC/S sheath. It was demonstrated that sulfur embedded in the pores of MPC is metastable small sulfur molecules of $S_{2\text{-}4}$ (S_2, S_3 and S_4) that have a chain-like structure instead of S_8 rings. Consequently, the S/(CNT@MPC) cathode showed a unique electrochemical behavior that exhibited a single discharge plateau at ~ 1.85 V (Figure 7a), instead of two distinguishable discharge plateaus, which is a similar phenomenon to that shown in the previous work discussed above.[46] As shown in Figure 7b, the S/(CNT@MPC) cathode showed a high initial specific capacity of 1670 mAh/g, an impressive cycling stability of 1149 mAh/g after 200 cycles, and a favorable high-rate capability of 800 mAh/g at 5 C. It was suggested that the excellent electrochemical properties of the S/(CNT@MPC) cathode could be attributed not only to an efficient 3-D network of electrical pathways for enhancing the reaction kinetics, but also to the space confinement of the carbon micropores on sulfur that prevents the formation of highly soluble lithium polysulfides (Li_2S_n, n = 4−8) by avoiding the transition between S_8 and S_4^{2-}.

As was discussed above, a core-shell-like structure that provides a closed environment for sulfur is one of the most promising concepts to improve the cycle life of Li/S cells by

isolating the sulfur from the liquid organic electrolyte. Hollow 1-D structured carbonaceous materials such as hollow carbon nanofibers and carbon nanotubes can be used as a host material that accommodates sulfur into their inner empty space by solution-based sulfur precipitation methods or a melt diffusion method with the help of capillary forces.[105-112] S. Moon *et al*. prepared hollow carbon nanowire (NW) arrays using anodic aluminum oxide (AAO) as a template material and then sulfur was inserted into the hollow space of the NWs, as shown in Figure 8a-e.[107] As a result, the uncommon monoclinic phase of sulfur encapsulated in hollow carbon wires (S@C NW) with a very thin carbon shell of about 3 nm was obtained with a high sulfur content of up to 81 wt.%. To fabricate the cathode, the prepared 1-D structured S@C NW composite array was attached to a substrate of 316 stainless steel (SS) by using conductive epoxy and an additional conductive platinum (Pt) layer between the S@C NW composite and the 316 SS substrate. A high discharge specific capacity of about 1200 mAh/g at the very high rate of 20 C was measured and a capacity retention of more than 75 % (with specific capacity of 1078 mAh/g at 1000th cycle) was shown even after 1000 cycles at 2.0 and 5.0 C (Figure 8f). It was suggested that the excellent electrochemical performance of the S@C NW composite cathode is due to: (1) the unique structure of the electrode that prevents the embedded sulfur from having direct contact with the electrolyte. The absence of the first discharge plateau related to the formation of soluble lithium polysulfide (shown in Figure 8g) may support this idea because soluble lithium polysulfide cannot form unless there is direct contact between sulfur and electrolyte; (2) the short electrical diffusion pathway through sulfur overcomes the insulating nature of sulfur. The Pt layer may help to enhance the electronic conductivity of the cathode as well; (3) a robust carbon coating layer which endures the volume expansion of sulfur during discharge. Despite the excellent electrochemical performance of the 1-D structured S@C NW

composite cathode, some remaining issues due to the uncommon electrode structure can potentially limit the practical usage of the 1-D structured S@C NW composite cathode. Especially, it was emphasized that the adhesion between the novel Pt current collector and the 1-D structured S@C NW nano-composite array can significantly influence the electrochemical performance of the cathode. Of course, the high price of a Pt current collector can significantly increase the cost of the Li/S cell.

In the case of the 1-D structured sulfur/C core-shell nano-composites with common electrode micro-structure, the reversible capacity of the cells trended downward for the first 100 ~ 200 cycles [105, 106, 108] unless additional strategies to stabilize the cycling of these Li/S cells were employed. G. Zheng *et al*. revealed one possible capacity fading mechanism of the 1-D structured sulfur/C core-shell nano-composite cathode using *ex-situ* TEM observations, and overcame it by introducing an amphiphilic polymer that modifies the carbon surface, rendering strong interactions between the nonpolar carbon and the polar Li_xS clusters.[108] Figure 9 shows the TEM images of the pristine and the discharged (at 0.2 C to 1.7 V) sulfur/ hollow carbon nano-fiber cathode without and with functionalization of the carbon surface using polyvinylpyrrolidone (PVP). As shown in Figures 9a and 9b, the inner core (identified as Li_2S) of the sulfur/ hollow carbon nano-fiber cathode without modification shrank away from the carbon wall along the length of the hollow carbon nanofiber compared to that of the pristine hollow carbon/sulfur cathode after the first discharge. This result was unexpected because the volume of sulfur should be increased instead of shrinking, when sulfur is lithiated (~ 80 % when Li_2S forms). To explain this phenomenon, it was suggested that the separation of Li_2S from the carbon wall was caused due to the leakage of intermediate polysulfides from the hollow carbon nanofibers into the electrolyte through the openings, resulting in the loss of electrical contact and

capacity decay. On the other hand, the sulfur/PVP modified hollow carbon nano-fiber cathode did not show the severe detachment of Li_2S from the carbon wall; instead, some small spots were observed that might be formed by localized detachment of Li_2S (Figure 9d). Consequently, the sulfur/PVP modified hollow carbon nano-fiber cathode showed significantly improved electrochemical performance. The initial specific capacity of the unmodified and the modified cathodes were similar (about 800 mAh/g) at 0.5 C, but the unmodified cathode showed a dramatic specific capacity decay with a discharge capacity of a little more than 500 mAh/g after 100 cycles, while the PVP-modified cathode showed a more stable capacity retention of over 80 % for more than 300 cycles. DFT simulation results suggested that the hydrophobic groups of PVP allow anchoring of the polysulfide species within the carbon matrix, which supports the *ex-situ* TEM observation and the electrochemical test results. According to the improved electrochemical performance of the sulfur/PVP modified hollow carbon nano-fiber cathode and a few more reports,[113-115] the polymer assisted sulfur/1-D structured carbon nano-composite concepts are fairly effective for improving the cycle life of the Li/S cell. The polymer assisted sulfur cathode will be discussed in a separate section.

A tube-in-tube carbon nanostructure (TTCN) with MWCNTs confined within hollow porous carbon nanotubes was prepared by Y. Zhao *et al*.[112] using a SiO_2 template coated on the surface of MWCNTs followed by carbon coating on the surface of SiO_2 and etching of SiO_2, in sequence. The prepared TTCN was used as the host material accommodating sulfur in the space between the outer hollow porous carbon nanotubes, which was simply prepared by a melt diffusion method. This unique structure was intended not only to provide an efficient electron pathway through both inner MWNTs and the outer porous carbon wall, but also to help suppressing the dissolution of lithium polysulfides into the electrolyte using the micro- and

meso-pores of the outer carbon nanotubes. The S-TTCN nano-composite cathode delivered a specific capacity of about 700 mAh/g at the third cycle (the first and second cycles were cycled at 0.5 A/g for activation of sulfur) and 647 mAh/g after 200 cycles with a low decay rate of 0.089% per cycle at the discharge specific current of 2 A/g. Rate capability test results showed discharge specific capacities of about 800, 750, 650, and 550 mAh/g when the cathode was cycled at 1.0, 2.0, 4.0, and 6.0 A/g, respectively, and then the discharge capacity recovered to 850 mAh/g when the test specific current was reduced back to 0.5 A/g, indicating good rate capability of the S-TTCN cathode.

As was discussed above, sulfur/1-D structured carbon nanocomposites have a structural advantage in terms of conductivity, because the continuous 1-D structure of conductive carbon is efficient for delivering electrons to the active sulfur particles in the whole cathode area. From the structural design point of view, sulfur can not only be placed on the surface of 1-D structured carbon, but can also be inserted into the inner space of 1-D structured carbon, in case of CNTs or hollow CNFs that have a hollow inner space. The nano-composite with embedded sulfur inside the 1-D structured carbon might be more effective for protecting sulfur against lithium polysulfide dissolution during cycling rather than the nano-composite with coated sulfur onto the 1-D structured carbon because of their less open structure. However, even if sulfur is embedded in the inner space of the 1-D structured carbon, lithium polysulfides formed during cycling can diffuse into the electrolyte through openings in the carbon outer layer that are used for the sulfur infiltration process. Thus, it seems that both designs need an additional strategy to improve the cycle life of the Li/S cell; i.e. employing micro- or mesoporous material or a polymer as protection layer, or doping 1-D structured carbon with nitrogen.

2.3 Sulfur-Polymer Nano-composites

As discussed above, sulfur-carbonaceous material composites are very promising due to the attractive physical and chemical properties of carbonaceous materials that can help to overcome the drawbacks of the sulfur cathode. However, the synthesis processes of carbon are normally conducted at a relatively high temperature (> 450 ^{o}C) which is much higher than the melting temperature of sulfur (~ 115 ^{o}C), thus the opportunity for synthesis of carbon structures without damage to the sulfur particles, especially closed carbon structures that encapsulate sulfur particles, is limited. Alternatively, a melt diffusion method is commonly used for sulfur insertion into the empty space of carbon structures through pores or an open structure of carbon, however the pores or open structure of carbon can potentially serve as a lithium polysulfide diffusion pathway into the liquid electrolyte during cycling, resulting in capacity decay of the Li/S cell. Because of the technical difficulty in synthesizing a sulfur encapsulating carbon nano-composite, alternate composite systems that can encapsulate sulfur have been intensively studied. Polymers have been considered as promising materials for sulfur-composite cathodes because various polymer processing methods, especially solvent based processes are feasible at processing temperatures below 100 ^{o}C allowing sulfur to maintain its structure as long as the solvent does not dissolve sulfur during the process. The advantage of an ambient-temperature polymerization process is that it allows the polymer to be useful for fabrication of a sulfur-encapsulated nano-structured composite without structural damage or loss of sulfur.

Generally, polymers are mechanically soft, so they are suitable for use as a matrix material for sulfur-based composites that will accommodate the volume expansion caused by the lithiation of sulfur particles. The mechanical stability of a polymer matrix helps to physically

confine sulfur in the structure during cycling without mechanical failure of the composite, so physical contact between encapsulated sulfur particles and liquid electrolyte can be avoided, which means that sulfur can be confined in the cathode effectively. Moreover, some polymers have functional groups or atoms such as nitrogen and oxygen, so they can act as sulfur immobilizers that chemically trap sulfur and lithium polysulfides.[90, 108, 116-118] For these reasons, rational design of polymer-coated or –assisted sulfur based nano-composites with proper choice of polymer should be helpful in overcoming the drawbacks of the sulfur cathode. Among many polymers, conducting polymers such as polyaniline (PANi),[113, 116, 119-121] polythiophene (PTs),[122, 123] polypyrrole (PPy),[115, 121, 124-131] poly(3,4-ethylenedioxythiophene) (PEDOT),[121, 132, 133] and so on[74, 134, 135] have been explored for use in the sulfur cathode. Compared to traditional polymers that are used for electrically passive applications due to their electrically insulating nature, conducting polymers are beneficial for the sulfur cathode, because the insulating nature of sulfur (and Li_2S) is one of the major drawbacks of the sulfur cathode that limits utilization of sulfur as an electrode material. Conjugated polymers are the most popular class of polymeric conductors that is represented by poly(p-phenylene),[136] PPy,[137] PTs[138] and its 3-methoxy- derivative[139] and PANi.[140] The common feature of the structure of conjugated polymers is polyconjugation in the π-system of their backbone (for polyaniline, this holds only in the case of a doped polymer) and they possess the electronic properties of metals while retaining the mechanical properties and processability of conventional polymers.[141] The scientific details of conducting polymers are available in review articles.[141-147]

[Figure 10]

A sulfur/PANi nanotube polymer backbone/sulfur nano-composite (SPANi-NT/S) was reported by L. Xiao *et al.*[116] The self-assembled PANi nanotubes were treated at 280 °C with

elemental sulfur, so elemental sulfur reacted with the unsaturated bonds in the polymer chains to form cross-linked, stereo-network structures. This is known as the “vulcanization reaction”.[148-150] The usual views on the mechanism of the vulcanization process are that the activity of sulfur liberated in *statu nascendi* is high enough to enable it to react with rubber and to create the spatial structure of the vulcanizate.[149, 150] As a result, a SPANI-NT/S nano-composite that is composed of a SPANi network with both inter- and/or intra-chain disulfide bond interconnectivity (chemically confined sulfur) and infused sulfur into the hollow voids (physically confined sulfur) was prepared. A possible structure for the SPANi-NT/S nano-composite is shown in Figure 10a. The prepared SPANi-NT/S nano-composite cathode was electrochemically tested at various C rates and it exhibited specific capacities of 837, 614, and 568 mAh/g after 100 cycles at the 0.1, 0.5, and 1.0 C rates, respectively, indicating a good rate capability of the SPANi-NT/S nano-composite cathode (Figure 10b). A long cycle life of a Li/S cell with good capacity retention of 76 % with respect to its specific capacity of the 100th cycle (432 mAh/g) after 500 cycles at the 1.0 C rate was also demonstrated. The author suggested several factors that might contribute to the good electrochemical performance of SPANi-NT/S nano-composite cathode such as: (1) the vulcanization process produces a three-dimensional, cross-linked SPANi network that provides molecular-level encapsulation of the sulfur compounds; (2) the polymer matrix SPANi functions as a self-breathing, flexible framework during charge/discharge to reduce stress and structural degradation; (3) the electropositive amine and imine groups on the SPANi chains further attract polysulfides through electrostatic forces, thereby reducing the displacement of sulfur during repeated cycling.[116]

A yolk-shell nano-architecture consists of PANi as the shell and sulfur as the core was synthesized through the coating of PANi on sulfur nanoparticles followed a heating process to

create void space in the PANi shell by reducing the size of sulfur particles using the vulcanization reaction that consumes some of the elemental sulfur from inside, and partial evaporation of the elemental sulfur.[120] The empty space in the PANI shell can help to accommodate the volumetric expansion of the sulfur during the lithiation process, thus, a yolk-shell nano-architecture can exhibit better mechanical stability during cycling as compared to a common core-shell nano-structure. The electrochemical performances of the pure sulfur, the common core-shell S/PANi and the yolk-shell S/PANi nano-composite cathodes were compared using a galvanostatic discharge-charge test at 0.2 C. The cycling stability of the common core-shell S/PANi cathode was slightly improved, compared to that of the pure sulfur cathode, however, the specific capacities of both pure sulfur and S/PANi core-shell nano-composite cathodes decayed very quickly and only delivered specific capacities of 124 and 280 mAh/g, respectively after 125 cycles. These results indicate that the PANi coating on the sulfur particles can improve the electrochemical performance of the sulfur cathode by enhancing the electrical conductivity of the cathode and by reducing lithium polysulfide dissolution into the liquid electrolyte, however, the protective coating integrity of the S/PANi core-shell nano-composite was not preserved during the volumetric expansion caused by lithiation of the sulfur core, thus polysulfides can eventually escape during cycling. In contrast, the yolk-shell S/PANi nano-composite cathode retained a stable specific capacity of 765 mAh/g after 200 cycles, corresponding to a capacity retention of 69.5 %, which was much higher than that of both pure sulfur and S/PANi core-shell nano-composite cathodes. The improved cycling stability verified that the mechanical stability of the PANi shell provided by the empty space to accommodate volume expansion of sulfur particles can help to stabilize the specific capacity more effectively during cycling. The structural stability of the PANi shell of the S/PANi yolk-shell nano-

composite was confirmed by *ex-situ* SEM observation of the cycled S/PANi core-shell and S/PANi yolk-shell nano-composite cathodes. In the SEM images, the PANi shells of the S/PANi yolk-shell nano-composite were still well preserved, whereas most PANi shells of the S/PANi core-shell nano-composite were cracked after only 5 cycles.

Another conducting polymer, polythiophene (PTH) was also used as a conductive composite matrix to form a sulfur/polythiophene (S/PTH) core-shell nano-structured composite.[122] After the introduction of PTH, a flake-like PTH shell with a thickness of about 20 ~ 30 nm formed on the surface of the sulfur particles, which was observed by SEM and TEM. To verify the effect of the PTH coating on the electrochemical performance of the sulfur cathode, galvanostatic charge-discharge cycle tests were conducted and the results revealed that the cycle life and rate capability of the Li/S cell were significantly improved after PTH coating. The initial capacities of S/PTH core-shell nano-structured cathode and bare sulfur cathode were 1119 and 1019 mAh/g, respectively, however, the reversible capacity of the bare sulfur cathode decreased to only 282 mAh/g after 80 cycles, corresponding to a capacity retention of about 28 %. In contrast, the S/PTH core-shell nano-structured cathode showed a much higher specific capacity of 830.2 mAh/g after 80 cycles, corresponding to an improved capacity retention of 74.2 %. Because PTH itself can be used as an active material for a Li rechargeable cell,[151] a galvanostatic test was conducted for a PTH cathode under the same test conditions to demonstrate the contribution of PTH to the specific capacity of the S/PTH core-shell nano-structured cathode. The measured specific capacity of the Li/PTH cell was only about 10 mAh/g, indicating the negligible capacity contribution of PTH to the specific capacity of the S/PTH core-shell nano-structured cathode. The specific capacity of the Li/PTH cell was much smaller than that reported previously because the charge reaction between PTH and Li ions mainly occurs between about

3.0 and 4.0 V,[151] which is higher than the upper limit of the voltage window for the galvanostatic cycling test for the S/PTH core-shell nano-structured cathode. To evaluate the rate capability of the bare sulfur and the S-PTH core-shell nano-structured cathodes, a rate capability test was conducted at various test specific currents from 100 to 1600 mA/g and then back to 100 mA/g. At a low specific current of 100 mA/g, the specific capacities of the bare sulfur and the S/PTH core-shell nano-structured composite cathodes were comparable, however, as the test specific current and the cycle number increased, the specific capacity of the bare sulfur cathode became much smaller than that of the S/PTH core-shell nano-structured composite cathode. After a rate test from 100 to 1600 mA/g, the specific capacity of the S/PTH core-shell nano-structured composite cathode remained at 811 mAh/g when the specific current returned to 100 mA/g, indicating improved cycling stability of the Li/S cell after PTH coating. The improved sulfur utilization, cycle life and rate capability of the S/PTH core-shell nano-structured composite cathode was mainly due to the conductive nature of the PTH shell that reduced the particle-to-particle contact resistance.

[Figure 11]

Ultrafine sulfur nano-particles with a size of about 10 to 20 nm were prepared using a membrane to form micro-droplets of S/CS_2 solution and PVP in ethanol (precipitant) as a wrapping ligand to prevent the sulfur aggregation.[132] As the particle size of sulfur is reduced, the length of both electron and Li ion conducting pathways through insulating sulfur are also reduced, thus reaction kinetics can be improved. Next, PEDOT was coated on the sulfur nano-particles to prevent lithium polysulfide dissolution into the liquid electrolyte by stably-limiting direct contact between sulfur and liquid electrolyte and improving the electrical conductivity of the electrode.[132] The TEM images (Figure 11a and 11b) showed that the obtained sulfur nano-

particles have a spherical shape with diameters ranging from 10 to 20 nm and an amorphous shell with a thickness of about 5 nm is formed on the sulfur nano-particles after PEDOT coating. Figure 11c shows the voltage profiles of the commercial sulfur (cp-S), the synthesized sulfur nano-particles (nano-S) and the sulfur encapsulated in PEDOT matrix (nano-S@PEDOT) cathodes. As shown in the voltage profiles, the nano-S@PEDOT cathode exhibited a much more flat and well-defined lower plateau at 2.0 V, while the other two cathodes showed slopes between 2.1 ~ 1.5 V. The author suggested that the shape change of the voltage profile after PEDOT coating was because the PEDOT matrix can help to trap freshly formed long chain polysulfides in their structure, thus the formation of insoluble Li_2S_2 and Li_2S layers that impede electrical conduction at the sites in contact with the conducting network can be suppressed before the complete transition from long chain lithium polysulfide to short chain lithium polysulfide. On the contrary, when the sulfur particles directly contacted the liquid electrolyte due to the lack of a protection layer, long chain polysulfides may be reduced to short chain polysulfides and even to insoluble and insulating Li_2S_2 and Li_2S near the contact sites, which may hinder the reduction of polysulfides far away from the contact sites, and thus lead to a rapid increase of polarization as the discharge proceeds.[132] The comparison of cycling results shown in Figure 11d indicates that the nano-S cell exhibited an initial discharge specific capacity of up to 1000 mAh/g, more than that of the CP-S cell (about 700 mAh/g), however both the CP-S and the nano-S cells showed drastic capacity fading at a test specific current of 400 mA/g. After 10 cycles, the specific capacities of the CP-S and the nano-S cathodes decreased to 69% and 55% of their initial specific capacities, respectively. On the other hand, the nano-S@PEDOT cathode showed the highest initial specific capacity of about 1117 mAh/g and the best capacity retention of about 83 % after 50 cycles. The test results verified that the strategies of the nano-S@PEDOT were fairly

effective for improving the electrochemical performance of the Li/S cell.

[Figure 12]

W. Li *et al*. studied the influence of different conducting polymers on the electrochemical performance of the sulfur cathode.[121] PEDOT, PPY, and PANi, three of the most well-known conducting polymers, were coated, respectively, onto monodisperse hollow sulfur nanospheres through a simple polymerization process. The structures of the PANi-S, the PPY-S, and the PEDOT-S electrodes were the same except for the polymer coatings on the hollow sulfur nanospheres (the coating thicknesses were also maintained the same, the electrochemical performances of conducting polymer coating with 20 nm thickness are discussed here.) to compare the effect of each conducting polymer on the electrochemical performance of Li/S cells, and the results of electrochemical tests are shown in Figure 12. The PANi-S, the PPY-S, and the PEDOT-S electrodes exhibited high initial specific discharge capacities of 1140, 1201 and 1165 mAh/g, respectively, at the 0.5 C rate, however, the PANi-S cell showed a relatively poor capacity retention of about 45 %, whereas the PPY-S and PEDOT-S cathodes exhibited capacity retentions of 60 and 67 %, respectively (Figure 12a). Because the functional groups in the polymers can affect the cycling stability of the sulfur cathode positively, *ab initio* simulations in the framework of DFT were performed to investigate the interaction between lithium polysulfide (Li_xS, $0 < x \leq 2$) species and the conducting polymers. The simulation results indicate that PEDOT has a much stronger binding energy (1.08 eV) with the lithium atom in Li-S than PANi (0.59 eV) and PPY (0.50 eV). Although the simulation results might not give us an absolute quantification of the binding strength, the experimentally demonstrated cycle life of the PANi-S, the PPY-S, and the PEDOT-S electrodes can be supported by a qualitative understanding of the influence of chemical bonding on the cycling stability of the sulfur cathode. The rate capability

test results and voltage profiles of the three cathodes (Figure 12b and 12c) clearly reveal that the rate capability of the cells were ordered as follows: PEDOT-S > PPY-S > PANI-S. At a high C-rate of 2.0 C, the PEDOT-S and PPY-S delivered reversible capacities of 858 and 789 mAh/g, which was higher than that of the PANI-S (666 mAh/g). As shown in Figure 12c, the voltage hysteresis between the discharge and the charge curves decreased in the order of PANI-S > PPY-S > PEDOT-S at both 0.2 C and 2.0 C. Because the structures of the three materials were the same, it was suggested that the rate capability of the cathodes was mainly determined by the conductivity of the polymer shell. The EIS test results supported the electrochemical test results, where the charge transfer resistance of the cathodes in order of PEDOT-S < PPY-S < PANi-S at different states of charge during the first discharge. Consequently, in this work, PEDOT was found to be the best choice to achieve a long cycle life and high-rate capability among the three conductive polymers, due to its strong binding energy with the lithium atom in Li-S, and better conductivity than those of the other conductive polymers.

It was emphasized previously that electrically conductive matrix materials for sulfur based composites are desired due to the insulating nature of sulfur and Li_2S. This is the reason that conducting polymers have been mainly considered for the sulfur cathode, among many polymers. However, as was discussed above, non-conductive PVP can also improve the cycle life of the Li/S cell by chemically trapping lithium polysulfides in the cathode during cycling.[108] A few works have been recently reported on developing polymer-sulfur cathodes with the non-conducting polymers such as PVP,[108] amylopectin[90] and polydopamine[117, 118] that are capable of chemically trapping lithium polysulfides. Because these polymers are not beneficial in terms of electronic conductivity, they were used as supporting materials to further improve the electrochemical performance of sulfur-carbon composite cathodes. W. Zhou *et al*. reported a

polydopamine coated, nitrogen-doped hollow carbon-sulfur double-layered core-shell structure that has multiple barriers to confine sulfur in the cathode.[117] As discussed in the sulfur/carbon nano-composites section, a nitrogen doped porous carbon shell can physically and chemically trap lithium polysulfides during cycling. However, pores in the carbon shell used for sulfur insertion into the hollow space can serve as a lithium polysulfide diffusion pathway to the electrolyte, thus a potential risk to lose sulfur from the electrode exists during cycling. To overcome this drawback, a nitrogen doped hollow carbon-sulfur cathode (NHC-S) was surrounded by an additional polydopamine shell layer (PDA-NHC-S), so the immobilization of lithium polysulfides was facilitated. Based on the results of galvanostatic charge-discharge testing at the 0.2 C rate, both the NHC-S and the PDA-NHC-S nano-composite cathodes delivered similar initial discharge capacities of 1141 and 1070 mAh/g, respectively. However, the specific capacity of the NHC-S cathode gradually decreased and showed about 600 mAh/g after 150 cycles. In contrast, the PDA-NHC-S composite cathode exhibited the best capacity retention of about 84 % after 150 cycles with a capacity of 900 mAh/g. To verify a long cycle life of the PDA-NHC-S composite cathode, it was also galvanostatically cycled at 0.6 C. The excellent cycle life of the PDA-NHC-S composite cathode was demonstrated with the specific capacity of 630 mAh/g after 600 cycles, corresponding to a capacity retention of 85.1 %.

In summary, polymers are useful as matrix materials for sulfur based nano-composites because many polymerization or polymer coating processes can be conducted at a relatively low temperature of less than 100 ^{o}C, which allows sulfur to maintain its structure as long as the solvent for the polymer processing does not dissolve sulfur. Therefore, sulfur encapsulated nano-structures with a polymer matrix can easily be prepared without structural damage or loss of sulfur. Among many polymers, electrically conducting polymers have been extensively studied

for sulfur cathodes to facilitate ion and charge transport. Moreover, various polymers can chemically trap sulfur and lithium polysulfides using their functional groups, thus, the cycle life of Li/S cells can be improved. In addition, polymers are mechanically soft, thus the volume expansion of sulfur particles caused by the lithiation process can be effectively accommodated, and stable protection against mechanical failure of the electrode, and lithium polysulfide dissolution can be provided. However, chemical and thermal stability of these polymers in organic electrolytes needs to be addressed for any commercial Li/S cell.

2.4 Other Sulfur Based Nano-composites

As discussed above, uniquely structured sulfur/carbonaceous material and sulfur/polymer nano-composites with promising electrochemical performance have been proposed as cathode materials for the Li/S cell in numerous papers. It is unquestioned that nano-structured sulfur/carbonaceous material and sulfur/polymer composites are in the mainstream of research on developing advanced Li/S cell cathodes, however, there are some other notable achievements for developing sulfur-based composite cathode systems such as sulfur/metal oxides[152-165] and sulfur/metal organic framework (MOF)[166] nano-composites and organosulfur compounds[167-177] for Li/S cells. These classes of sulfur-based nano-composite cathodes can offer new opportunities to improve the electrochemical properties of the Li/S cell.

Among them, sulfur/metal oxide nano-composites have attracted attention from researchers with a few different concepts to improve the cycle life of Li/S cells, *e.g.* absorbing materials to trap lithium polysulfides;[152-157] porous structured metal oxide as lithium polysulfide reservoirs[158-162] and insulating protection layers to suppress lithium polysulfide dissolution into

the liquid electrolyte.[163-165] In 2013, binary and ternary metal oxides such as La_2O_3,[152] Al_2O_3[153] and $Mg_{0.6}Ni_{0.4}O$[154] were proposed as absorbers of lithium polysulfides which were homogeneously distributed in the sulfur based composite. The metal oxides were intended to support the sulfur/carbon or sulfur/polymer nano-composites for further improvement in the electrochemical performance of Li/S cells, so they can also be regarded as additives. Although the working mechanisms as a lithium polysulfide absorber aren't clearly revealed in the papers, sulfur based nano-composite cathodes containing metal oxide additives showed higher reversible discharge capacity and better capacity retention than those of the sulfur based nano-composite cathodes without the metal oxides. The beneficial effect of $Mg_{0.6}Ni_{0.4}O$ as polysulfide absorber was demonstrated by SEM observation of both the cycled sulfur/PAN and the sulfur/PAN/$Mg_{0.6}Ni_{0.4}O$ cathodes. In the SEM image of the sulfur/PAN cathode, agglomeration of the composite particles in the cathode was clearly observed, whereas agglomeration was suppressed when $Mg_{0.6}Ni_{0.4}O$ was employed in the sulfur/PAN composite.[154]

Recently, the metallic oxide, Ti_4O_7 was reported as a component of a sulfur-based nano-composite by Q. Pang *et al.*[156] and X. Tao *et al.*[157] Magnéli Ti_4O_7 is a highly conductive oxide that exhibits a bulk metallic conductivity of 2×10^3 S/cm at 298 K[178] and it contains polar O-Ti-O units that have a high affinity for lithium polysulfides, thus it can bind lithium polysulfides.[156] Q. Pang et al. prepared a highly porous Magnéli Ti_4O_7, exhibiting a very high BET surface area of 290 m^2/g for efficient utilization of a polar surface for a strong lithium polysulfide binding effect as well as a physical confinement of sulfur and lithium polysulfide using its pores. Consequently, the sulfur/porous Ti_4O_7 nano-composite has multiple features for improving the electrochemical performance of the Li/S cell. To verify the effect of the porous Magnéli Ti_4O_7 host, a sulfur/Ti_4O_7 nano-composite cathode was prepared and galvanostatically tested between 1.8 V and 3.0 V. The

voltage profiles of the sulfur/Ti_4O_7 nano-composite cathode at different C-rates from 0.05 C to 1 C only showed a little increase in polarization with increasing rate, which indicates that the high electronic conductivity of the Ti_4O_7 host improved the rate capability without contribution to the capacity of the cell (only 6 mAh/g at the same test condition). The long cycle life of the sulfur/Ti_4O_7 (60 % S, Ti_4O_7-S/60) nano-composite cathode was demonstrated at the 2.0 C rate, with an initial specific capacity of 850 mAh/g and a capacity fade rate of only 0.06 % per cycle over 500 cycles. The excellent cycle life of the Ti_4O_7-S/60 cathode was attributed to not only physical confinement of sulfur and lithium polysulfides in the pores of the mesoporous Ti_4O_7, but also a polar surface for strong lithium polysulfide binding. To verify a polysulfide binding effect of Ti_4O_7, a sulfur/porous carbon nano-composite cathode was prepared, which has a similar BET surface area of about 260 m^2/g and sulfur content (60 %) in the composite. Compared to the fast capacity decay rate of the sulfur/carbon cathode (0.16% per cycle), the Ti_4O_7/S-60 cell showed good capacity retention with a fade rate as low as 0.08% per cycle over 250 cycles at 0.5 C. This result was supported by SEM observations of the electrodes after the first discharge that showed conformal Li_2S deposition on the particle surface of the Ti_4O_7/S-60 cathode, whereas the Li_2S on the carbon composite was broadly and nonspecifically distributed. DFT calculations and experimental characterizations such as XPS, and TEM with EDS conducted by X. Tao *et al*. also proved that the surface of Ti_4O_7 with abundant low coordinated Ti sites is favorable for the adsorption and selective deposition of the sulfur species, resulting in improved cycle life of the Li/S cell.[157]

[Figure 13]

A highly efficient polysulfide mediator, manganese dioxide (MnO_2) was reported by L. F. Nazar and co-workers in 2015.[155] They found that ultra-thin MnO_2 nanosheets can entrap lithium

polysulfide by the unique surface reaction chemistry of MnO_2, thus sulfur can be confined in the cathode during electrochemical cycling, resulting in good cycle life for the Li/S cell. For visual confirmation of polysulfide entrapment at specific discharge depths, electrochemical cells with sulfur/ketjen black (S/KB) and S/MnO_2 nanosheet cathodes were assembled in clear vials (Figure 13a) and the cells were galvanostatically discharged to 1.8 V at 0.05 C. As a result, the clear electrolyte in the S/KB cell changed to bright yellow-green on partial discharge of the cell over 4 h and the color of the electrolyte remained yellow until the end of discharge (12 h), indicating the existence of the solubilized lithium polysulfide in the electrolyte. In contrast, in the S/MnO_2 cell, the electrolyte exhibited only a faint yellow color at 4 h, demonstrating a relatively better trapping of lithium polysulfide compared to the S/KB cells. Interestingly, the electrolyte was rendered completely colorless at the fully discharged state, which means that the soluble lithium polysulfide was effectively converted to insoluble reduced species such as Li_2S_2 and Li_2S. A unique two step reaction chemistry of MnO_2 to mediate lithium polysulfide was proposed as follows: (1) thiosulfate groups are first created *in situ* by oxidation of initially formed soluble lithium polysulfide species on the surface of ultra-thin MnO_2 nanosheets. (Figure 13b); (2) As reduction proceeds, the surface thiosulfate groups are proposed to anchor newly formed soluble 'higher' polysulfides by catenating them to form polythionates and converting them to insoluble 'lower' polysulfides. (Figure 13c) The S/MnO_2 cell exhibited a long cycle life with an initial discharge capacity of up to 1300 mAh/g and 380 mAh/g after 1200 cycles at 0.2 C, which was attributed to active polythionate complexes on the surface of MnO_2 serving as an anchor and transfer mediator to confine sulfur in the cathode.

Porous nano-structured metal oxides such as silica[162] and titania[158-161], which have been widely studied for many applications (*e.g.*, microelectronics, chemical sensors and catalyst

substrates) are also notable as a component of sulfur based nano-composites for Li/S cell cathodes. The strategy of using porous metal oxides to improve the cycle life of the Li/S cell is technically the same as that of porous carbonaceous materials, which can be briefly described as physical confinement of sulfur and lithium polysulfides in micro-, meso- and macro pores during electrochemical cycling, the so-called polysulfide reservoir concept. One of the representative works was conducted by Ji *et al*., wherein mesoporous silica (SBA-15) was used as a lithium polysulfide reservoir. SBA-15 is well-ordered hexagonal silica with tunable large uniform pore sizes that exhibit high surface area, a large pore volume and highly hydrophilic surface properties.[179] SBA-15 was mixed with a meso-porous carbon/sulfur (SCM/S) nano-composite to form a SBA-15-SCM/S nano-composite and the composite was used as the active material for a sulfur cathode. The SCM/S and the SBA-15-SCM/S cathodes were galvanostatically cycled at 0.2 C and the results showed that similar initial capacities of the SMC/S and the SBA-15-SCM/S cells were obtained (920 and 960 mAh/g, respectively), however, the capacity of the SMC/S cathode decayed to less than 500 mAh/g after 40 cycles, whereas that of the SBA-15-SCM/S cathode was above 650 mAh/g. The Coulombic efficiency of the Li/S cell was also improved to about 98 % when SBA-15 was added, indicating that the existence of the SBA-15 can further improve cycle life of the SMC/S cell, as a result of sulfur polysulfide confinement.

Recently, a sulfur/metal organic framework (MOF) nano-composite cathode was reported by J. Zheng *et al*.[166] MOFs are an emerging class of porous materials constructed from metal-containing nodes (also known as secondary building units, or SBUs) and organic linkers.[180] MOFs are structurally and functionally tunable by organic ligand design and post-synthetic modification of the linker as well as the metal clusters and their coordination bonds. These inorganic-organic hybrid materials commonly offer very high porosity and large surface area,

thus it is reasonable that MOFs are considered as a porous structured host material for use in sulfur based nano-composites. In J. Zheng's work, a hierarchical porous structured Ni-MOF was synthesized with an extremely high BET surface area of 5243 m^2/g and a sulfur/Ni-MOF nano-composite that consisted of about 60 wt. % sulfur was obtained using a melt-diffusion method at 155 ^oC. After sulfur insertion, the BET surface area decreased to 514 m^2/g, which may indicate that the pores of Ni-MOF were filled with elemental sulfur. The prepared sulfur/Ni-MOF nano-composite was electrochemically evaluated as a Li/S cell cathode material and the results showed an initial specific capacity of about 689 mAh/g and a specific capacity of 611 mAh/g after 100 cycles at 0.1 C. Although the specific capacity of the sulfur/Ni-MOF nano-composite cathode was lower than that of sulfur/carbonaceous material nano-composite cathodes reported in the previous literature, which is probably due to the poor conductivity of Ni-MOF, it showed a good capacity retention of about 89 % after 100 cycles. The improved sulfur/Ni-MOF cell cycle life could be attributed to not only the porous structure of Ni-MOF, but also the strong interactions between the Lewis acidic Ni(II) center and the polysulfide soft Lewis base, which was confirmed by a DFT study.

Use of metal oxide materials as a protective coating layer to inhibit polysulfide dissolution into liquid electrolytes has been reported using alumina (Al_2O_3)[163, 164] or silica (SiO_x).[165] H. Kim *et al*. coated an Al_2O_3 layer onto the surface of a sulfur/carbon composite using rapid plasma enhanced atomic layer deposition (PEALD). Sulfur/activated carbon fibers (S/ACFs) were first prepared using a melt-diffusion method and they were cast onto a Ni current collector with a polyacrylic acid (PAA) binder. After casting and vacuum drying of the electrode, PEALD was conducted to form an Al_2O_3 layer on the electrode surface. Because of the low operating temperature of PEALD, evaporation of sulfur could be avoided during the Al_2O_3

coating. To verify the effect of the Al_2O_3 protective layer on the electrochemical performance of the Li/S cell, both the uncoated and coated S/ACFs nano-composite cathodes were galvanostatically cycled at 0.5 C at 70 ^oC to accelerate the polysulfide dissolution into the liquid electrolyte, intending faster cell degradation. As a result, the uncoated S/ACFs nano-composite cathode showed an initial specific capacity of about 900 mAh/g, whereas that of the Al_2O_3 coated S/ACFs nano-composite cathode (50-Al_2O_3 with thickness of Al_2O_3 in the range from 3 to 5 nm.) was around 400 mAh/g at 0.2 C, which might be caused by the Al_2O_3 layer increasing the electrode resistance. Although the initial capacity of the Al_2O_3 coated S/ACFs nano-composite cathode was smaller than that of the uncoated S/ACFs nano-composite cathode, it maintained a reversible capacity of above 300 mAh/g for 370 – 470 high-temperature cycles, whereas that of the uncoated S/ACFs nano-composite cathode deceased to below 50 mAh/g after 200 cycles. The stable cycling performance of the Al_2O_3 coated S/ACFs nano-composite cathode was supported by SEM observation of the both anode and cathode in the Al_2O_3 coated S/ACFs cell after 200 cycles, which showed a uniform morphology of cathode and a smooth surface of the Li foil anode. In contrast, the morphology of both anode and cathode in the uncoated S/ACFs cell were covered by large chunks of lithium sulfide. These results indicated that the Al_2O_3 coating can reduce lithium sulfide dissolution from the cathode, thus the shuttling effect of lithium polysulfides to the Li anode can be suppressed.

Organosulfur compounds which are one class of organic materials that contain sulfur in their chemical structure offer a novel class of sulfur cathode for the Li/S cell. Organosulfur compounds were reported by S. J. Visco *et al*. as alternative electrode materials for the high temperature sodium/sulfur cell to lower the operating temperature of the cell, in order to overcome the corrosion of the positive electrode container caused by the molten polysulfides at

the operation temperature of about 320 ~ 350 ^{o}C.[181] Since the lithium rechargeable cell became popular in the 1990s, various organosulfur compound cathodes have been investigated as active materials for the lithium rechargeable cell cathode.[167-177] The basic overall cell reaction of lithium/organosulfur compound cathodes can be expressed as:[167]

Positive electrode: $RSSR + 2e^{-} \rightarrow 2RS^{-}$

Negative electrode: $Li \rightarrow Li^{+} + e^{-}$

Overall: $2Li + RSSR \rightarrow 2LiSR$

where R is an organic moiety.

[Table 1]

In the context of searching for a new sulfur cathode system, organosulfur compound cathodes are attractive due to the advantages of polymer engineering such as a potentially low production cost and flexibility of material design for functionalization, because the physical and chemical properties or electrochemical behavior of organosulfur compound cathodes can vary depending on their molecular structure. However, some issues regarding the use of organosulfur compounds as cathode materials need to be addressed: (1) poor electrochemical kinetics that increase the polarization overpotential, resulting in loss of cell voltage. Thus, employing electronically conductive materials such as carbonaceous materials, conducting polymers and highly conductive metal powders might be needed to improve the electrochemical rate capability of organosulfur cathodes; (2) a low percentage of sulfur in the organosulfur compound causes a low specific energy of the Li/S cell, even if the organosulfur compound cathode exhibits a high specific capacity based on the mass of active sulfur. The weight corresponding to the electrochemically inactive portion of the molecules needs to be minimized to achieve a high specific energy of the Li/S cell; (3) physical and chemical stability of the organosulfur

compounds in electrochemical cell in the desired voltage window, which is necessary to obtain long cycle life. Some examples of organosulfur cathodes that have been studied for lithium rechargeable cells are given in Table 1.

[Figure 14]

Recently, a notable organosulfur compound cathode was reported by W. J. Chung *et al*., which was prepared by a facile 'inverse vulcanization' process to prepare chemically stable and processable polymeric materials through the direct copolymerization of elemental sulfur with vinylic monomers.[175] The inverse vulcanization process was described as the stabilization of polymeric sulfur against depolymerization by copolymerizing a large excess of sulfur with a modest amount of small-molecule dienes, whereas polydienes are cross-linked with a small fraction of sulfur to form synthetic rubber in the conventional vulcanization process. The copolymerization process of S_8 with 1,3-diisopropenylbenzene (DIB) *via* inverse vulcanization is described in Figure 14a. Briefly, sulfur powder was heated at 185 ^{o}C for the ring-opening polymerization (ROP) of S_8 and DIB was added directly to the molten sulfur medium while the temperature was maintained at 185 ^{o}C. The prepared poly(sulfur-*random*-1,3-diisopropenylbenzene) (poly(S-r-DIB)) material was employed as a cathode material for the Li/S cell. Among the poly(S-r-DIB) materials which had sulfur contents from 50 to 90 %, poly(S-r-DIB) with a very high sulfur content of 90 % was chosen as the Li/S cell cathode material. As shown in Figure 14b, cyclic voltammetry (CV) curves of both the S_8 and the poly(S-r-DIB) cathodes were very similar, which showed two distinguishable discharge peaks, indicating similar electrochemical behavior between the poly(S-r-DIB) and the S_8 cathodes. The poly(S-r-DIB) cathode (Figure 14c) exhibited a good cycle life with specific discharge capacities of about 1100 and 823 mAh/g at the first and the 100th cycle, respectively, at 0.1 C. Rate capability test

results showed reasonable capacity retention between 900-700 mAh/g from the range of 0.2 C to 1.0 C rates and a specific capacity of 400 mAh/g was obtained at the 2.0 C rate. The poly(S-r-DIB) cathode should be highlighted among many organosulfur compound cathodes due to its good electrochemical performance with an exceptionally high sulfur content of 90 % in the compound as well as simple, inexpensive and scalable synthesis procedure.

In summary, various kinds of metal oxides have been explored as a component of sulfur based composites in order to enhance the cycle life of the Li/S cell. The role of metal oxides in sulfur-based composite cathodes depends on the physical and chemical structure of the metal oxides, for example, Ti_4O_7 or MnO_2 can entrap sulfur and lithium polysulfides on their surface which is attributed to their unique surface chemistry; Al_2O_3 or SiO_x can be used as an insulating protection layer that suppress polysulfide dissolution into the liquid electrolyte; porous structured metal oxides can act as polysulfide reservoirs using the pores to physically trap lithium polysulfides. However, it should be noted that the nanostructured metal oxides which can be regarded as ‘additives’ not only can potentially increase the production cost of the cell, but also decrease the specific energy of the Li/S cell owing to the weight of metal oxide that does not contribute to specific capacity. In the case of organosulfur compound cathodes, although they can offer more alternative cathode systems for the Li/S cell, they need to be further investigated for practical use due to their poor reaction kinetics, uncertainty of thermal or chemical stability of organosulfur compounds in the temperature range for many battery applications and undesired ‘dead weight’ due to all of the remaining portions of the molecules except for the active sulfur.

3 Binders, Conducting Additives and Current

Collectors

Most investigations for developing advanced sulfur cathodes have mainly been focused on the design of active sulfur-based nano-composites. A significant amount of previous work successfully demonstrated that the design of the active sulfur-based nano-composites plays an important role in improving the electrochemical performance of the Li/S cell. In the sulfur cathode, however, 1~20 wt.% of the active material layer on the current collector is generally devoted to binder and conductive carbon, which means that they also greatly influence the cell performance. Therefore, it is necessary to extensively study the binder and conductive carbon additive as well as the current collector to optimize the architecture of the sulfur cathode. In the following section, various kinds of binder, conductive carbon additives as well as current collectors and their recent progress will be discussed.

3.1 Binders

The binder plays an important role in creating a durable electronically conductive network by maintaining connection among all electrode components during electrochemical cycling while allowing lithium ion transport into the internal electrode space. Mechanical failure of the sulfur cathode can occur during electrochemical cycling due to the volume expansion of sulfur particles up to 80 % (when Li_2S forms), which can cause a loss of electrical contact between active sulfur and the current collector, resulting in a decrease of specific capacity. Thus, the binder needs to act as a buffer material to accommodate the volume change of sulfur particles during cycling to maintain the electronic contact of all electrode components in order to achieve good utilization and cycle life. The binders can be categorized depending on the solvent that is used for

dissolving the binder: (1) binders used in aqueous systems; (2) binders used in organic solvent systems. The aqueous systems have advantages for mass production compared to organic solvent systems, because they use water as solvent which is inexpensive, safe and environmental friendly, whereas organic solvents are commonly toxic, flammable, and expensive. Poly(vinylidene difluoride) (PVDF) is the most common binder for both anode and cathode in conventional lithium ion cells due to its good adhesion properties with other electrode components,[182] and it has also been popularly used for sulfur cathodes. Nevertheless, some critical drawbacks have been noted that cause degradation of cell performance, *e.g.* PVDF cannot successfully accommodate the stress/strain caused by the volume change of sulfur particles due to its stiff nature; use of N-methyl-2-pyrrolidone (NMP) which is toxic and hard to evaporate due to its low vapor pressure (40 pa while that of water is 2300 pa at 20 ^{o}C) and high boiling point (~ 202 ^{o}C); the electrically insulating nature of PVDF increases the resistance of the cathode. For these reasons, many attempts have been made to develop alternative binder systems for the sulfur cathode.

Polyethylene oxide (PEO) is one of the representative binders, which is often used for Li/S cells[183, 184] instead of PVDF, because it can be dissolved in acetonitrile or propyl alcohol which are less toxic and easier to evaporate than NMP. However, electrode swelling was found to be extreme and the cause of capacity decrease due to a loss of electrical contact between sulfur and the current collector.[185] Recently, Lacey *et al*. reported that the sulfur cathode with a PEO-PVP composite binder system can improve the electrochemical performance over that of cathodes with the PVP binder or the PEO single binder systems.[186] It was previously demonstrated by Seh *et al*. that the PVP binder has a strong affinity with both Li_2S and lithium polysulfide, thus it can help to improve cycle life of the Li/S cell.[187] In Lacey's work, the sulfur

cathode with the PEO-PVP (8:2 by weight) composite binder system showed significant improvement in electrochemical performance with a specific capacity of about 1000 mAh/g after 50 cycles at 0.2 C, whereas the cathodes with the PEO and PVP binders showed about 900 mAh/g. Besides the chemical entrapment of lithium polysulfides, addition of PVP into the PEO binder allows PEO to be used in aqueous systems. Commonly, water-based slurries containing only PEO as the binder are extremely viscous,[186] so it is difficult to obtain a good laminate. However, the viscosity of the slurry can be greatly improved by adding PVP because PVP is a well-known polymer dispersant.

In general, aqueous system binders have great advantages such as their environmentally benign nature, low cost, and easy engineering of aqueous processes, which does not interfere with the advantages of the sulfur cathode. So, various aqueous binder systems such as gelatine[188, 189] nafion[190] polyacrylic acid (PAA)[118, 191] and styrene-butadiene rubber (SBR)[88, 192, 193] have been explored for Li/S cell. In 2013, L. Wang *et al*. designed a long-life sulfur cathode using a cross-linking reaction between polydopamine (PD) buffer on the surface of S/RGO nano-composite and PAA binder.[118] The PD coating layer on S/RGO nano-composite not only chemically traps lithium polysulfides during cycling, but also forms a strong covalent bond through the dehydration of the carboxyl group of PAA and the amino group of PD to produce a tertiary amide, resulting in improvement of the electrode stability. As a result, the PD coated S/RGO cathode with PAA binder exhibited a long cycle life with a specific capacity of 728 mAh/g after 500 cycles at a specific current of 0.5 A/g.

SBR is commonly used in combination with a thickening agent, carboxymethylcellulose (CMC), and the laminate with SBR-CMC composite binder shows strong adhesion to the current collector. The elastomeric nature of SBR is beneficial for accommodating stress (or strain)

caused by the volume change of sulfur particles during cycling, thus the structural integrity of the sulfur cathode can be enhanced, indicating that the electronic network of the sulfur cathode can be effectively maintained.[192] Consequently, the cycle life of the Li/S cell can be improved by replacing PVDF binder with the SBR-CMC composite binder, which was demonstrated in the previous research on the CTAB modified S-GO cathode with SBR-CMC binder that exhibited a long cycle life of a Li/S cell over 1500 cycles with an extremely low capacity decay rate (0.039 % per cycle) at 1.0 C discharge.[88]

Another water soluble binder, a carbonyl-β-cyclodextrin (C-β-CD) which exhibited a high solubility in water and strong bonding capability was reported by J. Wang *et al.*[194] By modifying the β-cyclodextrin (β-CD) through a partial oxidation reaction in H_2O_2 solution, the solubility of the C-β-CD in water at room temperature increased to approximately 100 times higher than that of the β-CD. The C-β-CD binder also showed strong adhesion strength and formed a gel film tightly wrapping the surface of the sulfur-based composite (based on the SEM images), which suppressed the aggregation of the sulfur composite during cycling. The sulfur cathode with C-β-CD binder showed a high initial capacity of about 1543 mAh/g and remained at 1456 mAh/g after 50 cycles at 0.2 C, whereas that of the sulfur cathodes with PVDF and PTFE binders decreased to about 900 mAh/g.

According to many researches on binder systems, binders certainly play an important part in achieving good electrochemical performance. Binders necessarily enable the maintenance of electronic contact between sulfur, conductive carbon and current collector against the volume change of sulfur particles during cycling. Among many binders, aqueous binder systems are beneficial for manufacturing of sulfur cathodes due to their environmentally benign nature, low cost and easy engineering of the process. Despite the advantages of new binder systems, none of

them have completely replaced the PVDF binder for the sulfur cathode yet, which might be due to a lack of understanding of new binders. Thus, additional effort for developing an advanced binder system is required for a practical Li/S cell.

3.2 Carbon Additives

Carbonaceous materials such as graphite, carbon black (CB), CNT and graphene are widely used as conductive additives for sulfur cathodes due to its high electrical conductivity, physical and chemical stability and environmentally benign nature. In general, carbon additives are not involved in the electrochemical reaction, but act as an electronic pathway to compensate for the poor electronic conductivity of sulfur, resulting in improvement of sulfur utilization and rate capability. However, because the weight of the carbon additive is ‘dead weight’ for the specific energy of the cell, the carbon content in the sulfur cathode needs to be minimized (typically less than 10 %). Therefore, the carbonaceous materials that have a high surface area or unique structure (*e.g.* wired structure) are favorable for providing an effective electronic pathway with a limited carbon amount.

Four different carbon blacks (Ketjen black EC-600JD, Super C65, Printex-XE2, and Printex-A) were employed as conductive carbon in sulfur cathode and electrochemically evaluated by A. Jozwiuk *et al*.[195] Each carbon black has a different BET surface area (Printex-A: 30 m^2/g, Super C65: 65 m^2/g, Printex XE-2: 1000 m^2/g and Ketjen black EC-600JD: 1400 m^2/g), thus the slurry concentration was varied to optimize the consistency of the blend. As a result, it was found that the carbon additive with a higher specific surface area can provide a higher specific capacity, but a brittle electrode was produced as the surface area of carbon increased. It

was suggested that it is beneficial to mix the carbon blacks with different surface areas for better performance and at the same time high stability.

Unique structured carbonaceous materials such as CNT,[55, 97] CNF[184, 196] and graphene[55] were also explored as conductive carbon additives. Because of their one or two dimensional continuous structure, they can provide very stable and effective electron conduction pathways. For example, a sulfur cathode with addition of CNF exhibited a higher specific capacity and better capacity retention than that of a sulfur cathode with carbon particles, because the CNFs provide a good conductive network with structural stability.[196] In the same regard, MWCNT is also helpful for improving the cycling performance and rate capability of sulfur electrodes.[97] When MWCNT was employed in the sulfur cathode as a conductive additive, lower charge transfer resistance was measured by EIS than for the sulfur cathode without MWCNT addition. The sulfur cathode with a graphene and CNT mixture exhibited about two times higher specific capacity at 0.2 C than the sulfur cathode with Super P.[55]

There is no doubt that the use of carbon additives in the sulfur cathode can significantly improve the electrochemical performance of Li/S cells. Therefore, it is important to choose the proper conductive carbon additives that can work well with the other cathode components in order to form a structurally homogeneous microstructure. Even though the use of unique structured carbonaceous materials such as CNT and graphene can improve the electrochemical performance of the sulfur cathode, these materials should be considered carefully because they can potentially increase the production cost of the sulfur cathode due to their high price.

3.3 Current Collector

The current collector is used for electronic connection between the active sulfur particles and the external terminals of the cell. The sulfur-based active material is generally pasted onto the current collector together with a polymer binder and conductive carbon additive, thus the geometry of the sulfur cathode is strongly influenced by that of the current collector. For various cell packaging types such as cylindrical, rectangular, pouch and coin type cells, the current collector needs to offer not only good surface conditions for obtaining strong adhesion strength to the laminate, but also the proper geometry with flexibility. Typically, aluminum (Al) thin foil is employed as the current collector for the sulfur cathode due to its chemical stability at the potential of the sulfur cathode, good electrical conductivity[197] and the relative ease of manufacturing thin foil. To improve the electrochemical performance of the sulfur cathode, various kinds of modified Al foils have been studied such as carbon coated Al foil, expanded metal mesh and surface etched Al foil.

Recently, three-dimensional (3-D) structured current collectors which can accommodate active sulfur particles and conductive carbon additives in their interior space they have been studied for use in the sulfur cathode. In the case of the sulfur cathode with a conventional Al foil current collector, the laminate composed of active sulfur powder, conductive carbon additive and polymer binder just sits on the Al foil, thus the only efficient channel for conducting electrons is associated with the conductive carbon. On the other hand, 3-D structured current collectors are beneficial for delivering electrons to (or from) the entire volume of the sulfur cathode because active sulfur particles are generally well-dispersed in the interior space of the current collector. Moreover, the porous structure of the sulfur cathode with a 3-D structured current collector can be used as a direct channel for the electrolyte to reach the inner space of the sulfur cathode, so Li ions in the electrolyte can reach the sulfur particles easily, resulting in the improvement of charge

transfer. Furthermore, the void space of the sulfur cathode with a 3-D structured current collector can accommodate the volume change of the sulfur particles, so better structural stability of the sulfur cathode can be obtained during electrochemical cycling. In 2013, A nano-cellular carbon (NC) current collector which has micro-meso-macro porous architecture was reported by A. Manthiram and co-worker.[198] In that work, it was demonstrated that the sulfur cathode with a NC current collector provided a high initial specific capacity of 1249 mAh/g with a good capacity retention of 71 % at 0.2 C after 50 cycles, whereas the sulfur cathode with conventional Al foil showed an initial capacity of 871 mAh/g with a capacity retention of less than 35 % after 50 cycles. It was suggested that the 3-D and porous structure of the NC current collector improves the electrical conductivity of the sulfur cathode, and further inhibits active material loss and the polysulfide shuttle effect *via* its porous structure that acts as the lithium polysulfide reservoir.

A 3-D structured Al foil current collector was employed for a sulfur cathode that accommodates a very high sulfur loading of about 7.0 mg/cm^2.[199] An initial capacity of this sulfur cathode with 3-D structured Al foil current collector was about 860 mAh/g at 0.1 C, whereas that of the conventional sulfur cathode was only about 534 mAh/g, even with a lower sulfur loading of about 4.6 mg/cm^2. A long cycle life of more than 1000 cycles was demonstrated with a graphene foam based 3-D structured flexible sulfur electrode.[200] Graphene foam (GF) was supported by a poly(dimethyl siloxane) (PDMS) coating on the surface of the GF to form a network while providing flexibility to the cathode. This flexible and bendable sulfur cathode exhibited much better cycleability and rate capability than those of a typical sulfur cathode.

Recent progress on 3-D current collectors is notable for improving the electrochemical performance of the sulfur cathode. They successfully accommodate a large amount of sulfur in their structure and the cathode showed improvement in sulfur utilization. However, suitability of

the current collector design for various cell casings, cost issues, and thickness or weight of the 3-D structured current collectors should be considered carefully for their use in practical high specific energy Li/S cells.

4 The Interlayer Concept

In 2012, A. Manthiram and co-worker reported a notable new concept of a cell component to improve the cycle life of the Li/S cell, which is called the 'interlayer'.[201] The interlayer is not a conventional component of the Li/S cell, however, this electrolyte-permeable interlayer is generally placed between the sulfur cathode and the separator, so it is in direct contact with the sulfur cathode. In the Manthiram's work, a bifunctional micro-porous carbon paper was added between the sulfur cathode and the separator, which can act not only as an "upper current collector", but also a "polysulfide stockroom". Because the interlayer is electronically connected to the sulfur cathode, electrons can be supplied to the lithium polysulfides trapped in the interlayer, thus lithium polysulfide can be reutilized at the surface of the interlayer. As a result, both the sulfur utilization and the capacity retention can be improved. The Li/S cell with a porous carbon interlayer showed a specific capacity over 1000 mAh/g after 100 cycles at the 1.0 C rate with an average Coulombic efficiency of 97.6 %, corresponding to specific capacity retention of 85 %.

Since Manthiram's work was reported, various interlayer materials such as polymer interlayers,[114, 202] carbonaceous material interlayers,[63, 83, 203-208] metallic interlayers[208, 209] and composite systems[208, 210] have been studied. In addition to the porous structure of the interlayer, a hydroxyl-functionalized porous carbon paper was proposed to further improve the functionality

of the interlayer to trap lithium polysulfides during cycling.[204] It was suggested that the hydrophilic groups and the micro-crack enhanced surface adsorption properties of the carbon promote bonding of sulfur species to the surface of the interlayer. A conductive polymer, PPy interlayer which was fabricated onto the surface of the sulfur cathode was also reported by G. Ma *et al*. The functional interlayer, composed of PPY nano-particles, can suppress lithium polysulfide dissolution into the liquid electrolyte and its shuttle owing to the adsorption effect of PPy for lithium polysulfides, thus the cycleability of the Li/S cell was greatly improved. The discharge specific capacity of the Li/S cell with the PPy interlayer on the sulfur cathode was 846 mAh/g after 200 cycles with an average Columbic efficiency of 94.2 % at the 0.2 C rate, while the specific capacity of a Li/S cell without the PPy interlayer was only 587 mAh/g after 100 cycles with an average Coulombic efficiency of 83.4 %.

Conductive carbon interlayers coated on the surface of the separator, facing the cathode side were also reported.[208] A doctor blade method with a slurry containing PVDF binder was employed to coat the separator with a conductive layer. Super P, Ketjen black and MWCNT were employed as interlayer materials and all the cells that employed the modified separators with those carbonaceous materials showed significant improvement as compared to the cell with an untreated separator. Among the Li/S cells with different types of carbon blacks, the cells with separators coated by Ketjen black or MWCNT showed better electrochemical performance than that of the cell with a separator coated by Super P. These carbons contributed to a higher electronic conductivity, resulting in enhancement of the polysulfide re-utilization at the surface of the interlayer on the separator. The cells with separators coated by Ketjen black or MWCNT exhibited about 760 mAh/g after 150 cycles at 0.2 C, whereas the cell with the separator coated by Super P and the cell with the untreated separator showed specific capacities of only little more

than 500 mAh/g and 300 mAh/g, respectively.

According to the previous work on the interlayer concept, employing the interlayer can significantly improve the electrochemical performance of Li/S cells. Their porous structure or chemical functionality can suppress the polysulfide shuttle effect by re-utilizing the polysulfides at the surface of the interlayer, resulting in the improvement of the electrochemical performance of the cell. However, the increase of cell weight caused by adding the interlayer and the additional electrolyte filling the pores should be taken into account in designing a high specific energy Li/S cell.

5 Summary and Outlook

As discussed in this chapter, the Li/S cell has been widely regarded as a front runner in the search for the next-generation rechargeable battery because the Li/S cell offers a theoretical specific energy of ~ 2600 Wh/kg under the assumption of complete Li_2S formation during the discharge process, which is much larger than that of the Li ion cell (500 ~ 600 Wh/kg). Moreover, the advantages of the Li/S cell such as the low cost of sulfur, a low environmental impact and a technical similarity to the fabrication of the Li ion cell are very attractive features for rechargeable cells beyond Li ion cells. However, the drawbacks associated with the sulfur cathode (*e.g.* a poor electrical conductivity of sulfur or Li_2S; dissolution of polysulfides into liquid electrolytes and the shuttle effect; the volume expansion of sulfur particles up to 80 %) limit the sulfur utilization and cycle life of the Li/S cell. Thus extensive studies on the continuing development of more advanced sulfur electrodes must be done in order to produce a practical Li/S cell.

Recently, significant progress in the sulfur cathode has been achieved by developing a rational design of the sulfur cathode composed of sulfur-based nano-composites as active materials, conductive additives and binders. Many strategies for the design of sulfur based nano-composites have been proposed to improve the electrochemical performance of sulfur cathodes, which can be summarized as follows: (1) fabrication of nano-sized sulfur not only to reduce the length of both electron and Li ion conducting pathways through insulating sulfur, but also to improve the structural stability against the volume change during electrochemical cycling; (2) sulfur-based nano-composites with conductive materials to improve the conductivity of the sulfur cathode; (3) sulfur based nano-composites with physical or chemical immobilizers to trap sulfur and polysulfides within the cathode during cycling; (4) suppression of stress (or strain) caused by the volume change of sulfur particles during cycling using voids in the porous structures or mechanically stable matrix materials. The sulfur based nano-composites designed with these strategies and their multiple combinations show great improvement in the electrochemical performance of the sulfur cathode and sulfur/carbonaceous materials and sulfur/conducting polymer nano-composite are represented among them. In addition to the sulfur-based active materials, there is no doubt that the conductive carbon additive, binder and current collector play important roles in improving the electrochemical performance of the sulfur cathode by constructing a good micro-structure of the sulfur cathode that can offer a good electrical conductivity and structural stability, although most of the attention of researchers has been focused on developing nano-structured sulfur active materials. The addition of an interlayer in the Li/S cell is also worth considering further for improving the cell performance.

[Figure 15]

Although many promising sulfur cathode systems have been reported recently, some

important issues still remain to be addressed before a practical Li/S cell is possible. First of all, both the sulfur loading and the sulfur content need to be significantly increased while maintaining good sulfur utilization and cycle life of the Li/S cell. For example, the specific capacity of the sulfur cathode estimated using the weight of the laminate is only half of the specific capacity normalized by the sulfur mass on the cathode, if the sulfur content in the laminate is 50 %, because the other 50 % is 'dead weight'. Moreover, the weights of the other cell components such as electrolyte, separator and Li foil are important, so the weight ratio between active sulfur and the sum of the other component weights has to be high enough to achieve a high specific energy Li/S cell, which means that a high weight of sulfur per unit area is essential. Unfortunately, most of the results reported in the previous works were obtained with low sulfur loading (commonly around 1 mg/cm^2 or less) or low sulfur contents (below 70 %), or the cell performance was evaluated without consideration of the weight of the other cell components, even in cases where the sulfur loading the sulfur cathodes was high. Figure 15 shows the performance of the Li/S cells reported in selected references, and indicates that only a few works have achieved high sulfur loading cathodes while maintaining reasonably high sulfur utilization, although the cycle life of the cells still needs to be improved for practical use. The green zone of the figure indicates the performance necessary for achieving a specific energy greater than that of a lithium ion cell.

In addition to the sulfur loading issue, the production cost of the sulfur cathode is important, especially if it requires expensive or toxic materials. Scalability, reliability and a simple production environment for the sulfur-based nano-composite also need to be addressed for the design of the sulfur cathode. In addition, the cell performance at various temperatures and the safety properties need to be evaluated and improved for a commercial Li/S cell. Therefore,

continuing research for the further development of the sulfur cathode system is necessary to address all of these issues. However, we believe that the intensive effort of the battery community will overcome the existing challenges and eventually produce practical high specific energy Li/S cells.

6 References

1. T. Nagaura and K. Tozawa, *Prog. Batteries Sol. Cells*, 1990, 9, 209.
2. *Electrochemical Energy Storage Technical Team Roadmap*, U.S. DRIVE Partnership/U.S. Department of Energy: Washington, DC, 2013.
3. K. Mizushima, P. C. Jones, P. J. Wiseman and J. B. Goodenough, *Solid State Ionics*, 1981, 3–4, 171-174.
4. H. Danuta and U. Juliusz, Google Patents, 1962.
5. E. J. Cairns and H. Shimotake, *Science*, 1969, 164, 1347-1355.
6. X. Ji and L. F. Nazar, *Journal of Materials Chemistry*, 2010, 20, 9821-9826.
7. G. Jeong, Y.-U. Kim, H. Kim, Y.-J. Kim and H.-J. Sohn, *Energy & Environmental Science*, 2011, 4, 1986-2002.
8. Z. Liu, W. Fu and C. Liang, in *Handbook of Battery Materials*, Wiley-VCH Verlag GmbH & Co. KGaA, 2011, DOI: 10.1002/9783527637188.ch24, pp. 811-840.
9. P. G. Bruce, S. A. Freunberger, L. J. Hardwick and J.-M. Tarascon, *Nat Mater*, 2012, 11, 19-29.
10. S. Evers and L. F. Nazar, *Accounts of Chemical Research*, 2013, 46, 1135-1143.
11. Y. Yang, G. Zheng and Y. Cui, *Chemical Society Reviews*, 2013, 42, 3018-3032.
12. L. F. Nazar, M. Cuisinier and Q. Pang, *MRS Bulletin*, 2014, 39, 436-442.
13. G. Xu, B. Ding, J. Pan, P. Nie, L. Shen and X. Zhang, *Journal of Materials Chemistry A*, 2014, 2, 12662-12676.
14. Z. Lin and C. Liang, *Journal of Materials Chemistry A*, 2015, 3, 936-958.
15. L. Ma, K. E. Hendrickson, S. Wei and L. A. Archer, *Nano Today*, 2015, 10, 315-338.
16. S. Wu, R. Ge, M. Lu, R. Xu and Z. Zhang, *Nano Energy*, 2015, 15, 379-405.
17. M.-K. Song, E. J. Cairns and Y. Zhang, *Nanoscale*, 2013, 5, 2186-2204.
18. D.-W. Wang, Q. Zeng, G. Zhou, L. Yin, F. Li, H.-M. Cheng, I. R. Gentle and G. Q. M. Lu, *Journal of Materials Chemistry A*, 2013, 1, 9382-9394.
19. L. Chen and L. L. Shaw, *Journal of Power Sources*, 2014, 267, 770-783.
20. D. Bresser, S. Passerini and B. Scrosati, *Chemical Communications*, 2013, 49, 10545-10562.

21. J. R. Akridge, Y. V. Mikhaylik and N. White, *Solid State Ionics*, 2004, 175, 243-245.
22. X. He, J. Ren, L. Wang, W. Pu, C. Jiang and C. Wan, *Journal of Power Sources*, 2009, 190, 154-156.
23. R. Elazari, G. Salitra, Y. Talyosef, J. Grinblat, C. Scordilis-Kelley, A. Xiao, J. Affinito and D. Aurbach, *Journal of The Electrochemical Society*, 2010, 157, A1131-A1138.
24. Y. Yang, G. Zheng, S. Misra, J. Nelson, M. F. Toney and Y. Cui, *Journal of the American Chemical Society*, 2012, 134, 15387-15394.
25. Y. V. Mikhaylik and J. R. Akridge, *Journal of The Electrochemical Society*, 2004, 151, A1969-A1976.
26. H. Chen, C. Wang, W. Dong, W. Lu, Z. Du and L. Chen, *Nano Letters*, 2015, 15, 798-802.
27. C. Nan, Z. Lin, H. Liao, M.-K. Song, Y. Li and E. J. Cairns, *Journal of the American Chemical Society*, 2014, 136, 4659-4663.
28. X. H. Liu, L. Zhong, S. Huang, S. X. Mao, T. Zhu and J. Y. Huang, *ACS Nano*, 2012, 6, 1522-1531.
29. J. Y. Huang, L. Zhong, C. M. Wang, J. P. Sullivan, W. Xu, L. Q. Zhang, S. X. Mao, N. S. Hudak, X. H. Liu, A. Subramanian, H. Fan, L. Qi, A. Kushima and J. Li, *Science*, 2010, 330, 1515-1520.
30. C. K. Chan, H. Peng, G. Liu, K. McIlwrath, X. F. Zhang, R. A. Huggins and Y. Cui, *Nat Nano*, 2008, 3, 31-35.
31. L. Su, Y. Jing and Z. Zhou, *Nanoscale*, 2011, 3, 3967-3983.
32. K. S. W. Sing, D. H. Everett, R. A. W. Haul, L. Moscou, R. A. Pierotti, J. Rouquerol and T. Siemieniewska, *Pure and Applied Chemistry*, 1985, 57, 603-619.
33. J. Lee, J. Kim and T. Hyeon, *Advanced Materials*, 2006, 18, 2073-2094.
34. Z. Hu, M. P. Srinivasan and Y. Ni, *Advanced Materials*, 2000, 12, 62-65.
35. A. Ahmadpour and D. D. Do, *Carbon*, 1996, 34, 471-479.
36. H. Marsh and B. Rand, *Carbon*, 1971, 9, 63-77.
37. A. Oya, S. Yoshida, J. Alcaniz-Monge and A. Linares-Solano, *Carbon*, 1995, 33, 1085-1090.
38. N. Patel, K. Okabe and A. Oya, *Carbon*, 2002, 40, 315-320.
39. R. W. Pekala, *J Mater Sci*, 1989, 24, 3221-3227.
40. T. Kyotani, T. Nagai, S. Inoue and A. Tomita, *Chemistry of Materials*, 1997, 9, 609-615.
41. J. H. Knox, B. Kaur and G. R. Millward, *Journal of Chromatography A*, 1986, 352, 3-25.
42. J. L. Wang, J. Yang, J. Y. Xie, N. X. Xu and Y. Li, *Electrochemistry Communications*, 2002, 4, 499-502.
43. J. Wang, L. Liu, Z. Ling, J. Yang, C. Wan and C. Jiang, *Electrochimica Acta*, 2003, 48, 1861-1867.
44. C. Liang, N. J. Dudney and J. Y. Howe, *Chemistry of Materials*, 2009, 21, 4724-4730.
45. X. Ji, K. T. Lee and L. F. Nazar, *Nat Mater*, 2009, 8, 500-506.
46. B. Zhang, X. Qin, G. R. Li and X. P. Gao, *Energy & Environmental Science*, 2010, 3, 1531-1537.
47. G. He, X. Ji and L. Nazar, *Energy & Environmental Science*, 2011, 4, 2878-2883.
48. M. Rao, W. Li and E. J. Cairns, *Electrochemistry Communications*, 2012, 17, 1-5.
49. G. He, S. Evers, X. Liang, M. Cuisinier, A. Garsuch and L. F. Nazar, *ACS Nano*, 2013, 7, 10920-10930.
50. J. Kim, D.-J. Lee, H.-G. Jung, Y.-K. Sun, J. Hassoun and B. Scrosati, *Advanced*

Functional Materials, 2013, 23, 1076-1080.
51. K. Zhang, Q. Zhao, Z. Tao and J. Chen, *Nano Res.*, 2013, 6, 38-46.
52. N. Jayaprakash, J. Shen, S. S. Moganty, A. Corona and L. A. Archer, *Angewandte Chemie International Edition*, 2011, 50, 5904-5908.
53. T. Xu, J. Song, M. L. Gordin, H. Sohn, Z. Yu, S. Chen and D. Wang, *ACS Applied Materials & Interfaces*, 2013, 5, 11355-11362.
54. D. S. Jung, T. H. Hwang, J. H. Lee, H. Y. Koo, R. A. Shakoor, R. Kahraman, Y. N. Jo, M.-S. Park and J. W. Choi, *Nano Letters*, 2014, 14, 4418-4425.
55. D. Lv, J. Zheng, Q. Li, X. Xie, S. Ferrara, Z. Nie, L. B. Mehdi, N. D. Browning, J.-G. Zhang, G. L. Graff, J. Liu and J. Xiao, *Advanced Energy Materials*, 2015, DOI: 10.1002/aenm.201402290, n/a-n/a.
56. J. T. Lee, Y. Zhao, S. Thieme, H. Kim, M. Oschatz, L. Borchardt, A. Magasinski, W.-I. Cho, S. Kaskel and G. Yushin, *Advanced Materials*, 2013, 25, 4573-4579.
57. Z. Li, Y. Jiang, L. Yuan, Z. Yi, C. Wu, Y. Liu, P. Strasser and Y. Huang, *ACS Nano*, 2014, 8, 9295-9303.
58. Z. Li, L. Yuan, Z. Yi, Y. Sun, Y. Liu, Y. Jiang, Y. Shen, Y. Xin, Z. Zhang and Y. Huang, *Advanced Energy Materials*, 2014, 4, n/a-n/a.
59. M.-S. Park, B. O. Jeong, T. J. Kim, S. Kim, K. J. Kim, J.-S. Yu, Y. Jung and Y.-J. Kim, *Carbon*, 2014, 68, 265-272.
60. Z. Li and L. Yin, *ACS Applied Materials & Interfaces*, 2015, 7, 4029-4038.
61. D.-W. Wang, G. Zhou, F. Li, K.-H. Wu, G. Q. Lu, H.-M. Cheng and I. R. Gentle, *Physical Chemistry Chemical Physics*, 2012, 14, 8703-8710.
62. C.-P. Yang, Y.-X. Yin, H. Ye, K.-C. Jiang, J. Zhang and Y.-G. Guo, *ACS Applied Materials & Interfaces*, 2014, 6, 8789-8795.
63. J. Song, M. L. Gordin, T. Xu, S. Chen, Z. Yu, H. Sohn, J. Lu, Y. Ren, Y. Duan and D. Wang, *Angewandte Chemie*, 2015, 127, 4399-4403.
64. R. Demir-Cakan, M. Morcrette, F. Nouar, C. Davoisne, T. Devic, D. Gonbeau, R. Dominko, C. Serre, G. Férey and J.-M. Tarascon, *Journal of the American Chemical Society*, 2011, 133, 16154-16160.
65. H. B. Wu, S. Wei, L. Zhang, R. Xu, H. H. Hng and X. W. Lou, *Chemistry – A European Journal*, 2013, 19, 10804-10808.
66. W. Bao, Z. Zhang, C. Zhou, Y. Lai and J. Li, *Journal of Power Sources*, 2014, 248, 570-576.
67. L. Ji, M. Rao, H. Zheng, L. Zhang, Y. Li, W. Duan, J. Guo, E. J. Cairns and Y. Zhang, *Journal of the American Chemical Society*, 2011, 133, 18522-18525.
68. H. Wang, Y. Yang, Y. Liang, J. T. Robinson, Y. Li, A. Jackson, Y. Cui and H. Dai, *Nano Letters*, 2011, 11, 2644-2647.
69. S. Evers and L. F. Nazar, *Chemical Communications*, 2012, 48, 1233-1235.
70. N. Li, M. Zheng, H. Lu, Z. Hu, C. Shen, X. Chang, G. Ji, J. Cao and Y. Shi, *Chemical Communications*, 2012, 48, 4106-4108.
71. H.-J. Peng, J. Liang, L. Zhu, J.-Q. Huang, X.-B. Cheng, X. Guo, W. Ding, W. Zhu and Q. Zhang, *ACS Nano*, 2014, 8, 11280-11289.
72. H.-J. Peng, J.-Q. Huang, M.-Q. Zhao, Q. Zhang, X.-B. Cheng, X.-Y. Liu, W.-Z. Qian and F. Wei, *Advanced Functional Materials*, 2014, 24, 2772-2781.
73. J.-Z. Wang, L. Lu, M. Choucair, J. A. Stride, X. Xu and H.-K. Liu, *Journal of Power Sources*, 2011, 196, 7030-7034.

74. L. Yin, J. Wang, F. Lin, J. Yang and Y. Nuli, *Energy & Environmental Science*, 2012, 5, 6966-6972.
75. H. Sun, G.-L. Xu, Y.-F. Xu, S.-G. Sun, X. Zhang, Y. Qiu and S. Yang, *Nano Res.*, 2012, 5, 726-738.
76. L. Zhang, L. Ji, P.-A. Glans, Y. Zhang, J. Zhu and J. Guo, *Physical Chemistry Chemical Physics*, 2012, 14, 13670-13675.
77. R. Chen, T. Zhao, J. Lu, F. Wu, L. Li, J. Chen, G. Tan, Y. Ye and K. Amine, *Nano Letters*, 2013, 13, 4642-4649.
78. T. Lin, Y. Tang, Y. Wang, H. Bi, Z. Liu, F. Huang, X. Xie and M. Jiang, *Energy & Environmental Science*, 2013, 6, 1283-1290.
79. G. Zhou, L.-C. Yin, D.-W. Wang, L. Li, S. Pei, I. R. Gentle, F. Li and H.-M. Cheng, *ACS Nano*, 2013, 7, 5367-5375.
80. C. Zu and A. Manthiram, *Advanced Energy Materials*, 2013, 3, 1008-1012.
81. Y. Qiu, W. Li, W. Zhao, G. Li, Y. Hou, M. Liu, L. Zhou, F. Ye, H. Li, Z. Wei, S. Yang, W. Duan, Y. Ye, J. Guo and Y. Zhang, *Nano Letters*, 2014, 14, 4821-4827.
82. X. Wang, Z. Zhang, Y. Qu, Y. Lai and J. Li, *Journal of Power Sources*, 2014, 256, 361-368.
83. J. Xu, J. Shui, J. Wang, M. Wang, H.-K. Liu, S. X. Dou, I.-Y. Jeon, J.-M. Seo, J.-B. Baek and L. Dai, *ACS Nano*, 2014, 8, 10920-10930.
84. M.-Q. Zhao, Q. Zhang, J.-Q. Huang, G.-L. Tian, J.-Q. Nie, H.-J. Peng and F. Wei, *Nat Commun*, 2014, 5.
85. L. Zhou, X. Lin, T. Huang and A. Yu, *Journal of Materials Chemistry A*, 2014, 2, 5117-5123.
86. H. Li, X. Yang, X. Wang, M. Liu, F. Ye, J. Wang, Y. Qiu, W. Li and Y. Zhang, *Nano Energy*, 2015, 12, 468-475.
87. C. Wang, X. Wang, Y. Wang, J. Chen, H. Zhou and Y. Huang, *Nano Energy*, 2015, 11, 678-686.
88. M.-K. Song, Y. Zhang and E. J. Cairns, *Nano Letters*, 2013, 13, 5891-5899.
89. Z. Wang, Y. Dong, H. Li, Z. Zhao, H. Bin Wu, C. Hao, S. Liu, J. Qiu and X. W. Lou, *Nat Commun*, 2014, 5.
90. W. Zhou, H. Chen, Y. Yu, D. Wang, Z. Cui, F. J. DiSalvo and H. D. Abruña, *ACS Nano*, 2013, 7, 8801-8808.
91. B. Wang, S. M. Alhassan and S. T. Pantelides, *Physical Review Applied*, 2014, 2, 034004.
92. Z. R. Ismagilov, A. E. Shalagina, O. Y. Podyacheva, A. V. Ischenko, L. S. Kibis, A. I. Boronin, Y. A. Chesalov, D. I. Kochubey, A. I. Romanenko, O. B. Anikeeva, T. I. Buryakov and E. N. Tkachev, *Carbon*, 2009, 47, 1922-1929.
93. C. Tang, Q. Zhang, M.-Q. Zhao, J.-Q. Huang, X.-B. Cheng, G.-L. Tian, H.-J. Peng and F. Wei, *Advanced Materials*, 2014, 26, 6100-6105.
94. Z. Wang, X. Niu, J. Xiao, C. Wang, J. Liu and F. Gao, *RSC Advances*, 2013, 3, 16775-16780.
95. Z. W. Seh, H. Wang, P.-C. Hsu, Q. Zhang, W. Li, G. Zheng, H. Yao and Y. Cui, *Energy & Environmental Science*, 2014, 7, 672-676.
96. J. Guo, Z. Yang, Y. Yu, H. D. Abruña and L. A. Archer, *Journal of the American Chemical Society*, 2013, 135, 763-767.
97. S.-C. Han, M.-S. Song, H. Lee, H.-S. Kim, H.-J. Ahn and J.-Y. Lee, *Journal of The Electrochemical Society*, 2003, 150, A889-A893.

98. L. Yuan, H. Yuan, X. Qiu, L. Chen and W. Zhu, *Journal of Power Sources*, 2009, 189, 1141-1146.
99. L. Ji, M. Rao, S. Aloni, L. Wang, E. J. Cairns and Y. Zhang, *Energy & Environmental Science*, 2011, 4, 5053-5059.
100. J.-j. Chen, Q. Zhang, Y.-n. Shi, L.-l. Qin, Y. Cao, M.-s. Zheng and Q.-f. Dong, *Physical Chemistry Chemical Physics*, 2012, 14, 5376-5382.
101. Y.-S. Su, Y. Fu and A. Manthiram, *Physical Chemistry Chemical Physics*, 2012, 14, 14495-14499.
102. S. Xin, L. Gu, N.-H. Zhao, Y.-X. Yin, L.-J. Zhou, Y.-G. Guo and L.-J. Wan, *Journal of the American Chemical Society*, 2012, 134, 18510-18513.
103. J.-Q. Huang, H.-J. Peng, X.-Y. Liu, J.-Q. Nie, X.-B. Cheng, Q. Zhang and F. Wei, *Journal of Materials Chemistry A*, 2014, 2, 10869-10875.
104. L. Wang, Y. Zhao, M. L. Thomas and H. R. Byon, *Advanced Functional Materials*, 2014, 24, 2248-2252.
105. J. Guo, Y. Xu and C. Wang, *Nano Letters*, 2011, 11, 4288-4294.
106. G. Zheng, Y. Yang, J. J. Cha, S. S. Hong and Y. Cui, *Nano Letters*, 2011, 11, 4462-4467.
107. S. Moon, Y. H. Jung, W. K. Jung, D. S. Jung, J. W. Choi and D. K. Kim, *Advanced Materials*, 2013, 25, 6547-6553.
108. G. Zheng, Q. Zhang, J. J. Cha, Y. Yang, W. Li, Z. W. Seh and Y. Cui, *Nano Letters*, 2013, 13, 1265-1270.
109. Z. Xiao, Z. Yang, H. Nie, Y. Lu, K. Yang and S. Huang, *Journal of Materials Chemistry A*, 2014, 2, 8683-8689.
110. S. Chen, X. Huang, H. Liu, B. Sun, W. Yeoh, K. Li, J. Zhang and G. Wang, *Advanced Energy Materials*, 2014, 4, n/a-n/a.
111. H.-J. Peng, T.-Z. Hou, Q. Zhang, J.-Q. Huang, X.-B. Cheng, M.-Q. Guo, Z. Yuan, L.-Y. He and F. Wei, *Advanced Materials Interfaces*, 2014, 1, n/a-n/a.
112. Y. Zhao, W. Wu, J. Li, Z. Xu and L. Guan, *Advanced Materials*, 2014, 26, 5113-5118.
113. F. Wu, J. Chen, L. Li, T. Zhao and R. Chen, *The Journal of Physical Chemistry C*, 2011, 115, 24411-24417.
114. J.-Q. Huang, Q. Zhang, S.-M. Zhang, X.-F. Liu, W. Zhu, W.-Z. Qian and F. Wei, *Carbon*, 2013, 58, 99-106.
115. C. Wang, W. Wan, J.-T. Chen, H.-H. Zhou, X.-X. Zhang, L.-X. Yuan and Y.-H. Huang, *Journal of Materials Chemistry A*, 2013, 1, 1716-1723.
116. L. Xiao, Y. Cao, J. Xiao, B. Schwenzer, M. H. Engelhard, L. V. Saraf, Z. Nie, G. J. Exarhos and J. Liu, *Advanced Materials*, 2012, 24, 1176-1181.
117. W. Zhou, X. Xiao, M. Cai and L. Yang, *Nano Letters*, 2014, 14, 5250-5256.
118. L. Wang, D. Wang, F. Zhang and J. Jin, *Nano Letters*, 2013, 13, 4206-4211.
119. G.-C. Li, G.-R. Li, S.-H. Ye and X.-P. Gao, *Advanced Energy Materials*, 2012, 2, 1238-1245.
120. W. Zhou, Y. Yu, H. Chen, F. J. DiSalvo and H. D. Abruña, *Journal of the American Chemical Society*, 2013, 135, 16736-16743.
121. W. Li, Q. Zhang, G. Zheng, Z. W. Seh, H. Yao and Y. Cui, *Nano Letters*, 2013, 13, 5534-5540.
122. F. Wu, J. Chen, R. Chen, S. Wu, L. Li, S. Chen and T. Zhao, *The Journal of Physical Chemistry C*, 2011, 115, 6057-6063.
123. F. Wu, S. Wu, R. Chen, J. Chen and S. Chen, *Electrochemical and Solid-State Letters*,

2010, 13, A29-A31.
124. Y. Fu and A. Manthiram, *Chemistry of Materials*, 2012, 24, 3081-3087.
125. Y. Fu and A. Manthiram, *The Journal of Physical Chemistry C*, 2012, 116, 8910-8915.
126. F. Wu, J. Chen, L. Li, T. Zhao, Z. Liu and R. Chen, *ChemSusChem*, 2013, 6, 1438-1444.
127. G. Ma, Z. Wen, J. Jin, Y. Lu, K. Rui, X. Wu, M. Wu and J. Zhang, *Journal of Power Sources*, 2014, 254, 353-359.
128. J. Wang, J. Chen, K. Konstantinov, L. Zhao, S. H. Ng, G. X. Wang, Z. P. Guo and H. K. Liu, *Electrochimica Acta*, 2006, 51, 4634-4638.
129. X. Liang, Y. Liu, Z. Wen, L. Huang, X. Wang and H. Zhang, *Journal of Power Sources*, 2011, 196, 6951-6955.
130. Y. Zhang, Z. Bakenov, Y. Zhao, A. Konarov, T. N. L. Doan, M. Malik, T. Paron and P. Chen, *Journal of Power Sources*, 2012, 208, 1-8.
131. M. Sun, S. Zhang, T. Jiang, L. Zhang and J. Yu, *Electrochemistry Communications*, 2008, 10, 1819-1822.
132. H. Chen, W. Dong, J. Ge, C. Wang, X. Wu, W. Lu and L. Chen, *Sci. Rep.*, 2013, 3.
133. Y. Yang, G. Yu, J. J. Cha, H. Wu, M. Vosgueritchian, Y. Yao, Z. Bao and Y. Cui, *ACS Nano*, 2011, 5, 9187-9193.
134. J. Wang, C. Lv, Y. Zhang, L. Deng and Z. Peng, *Electrochimica Acta*, 2015, 165, 136-141.
135. J. Wang, J. Yang, C. Wan, K. Du, J. Xie and N. Xu, *Advanced Functional Materials*, 2003, 13, 487-492.
136. D. M. Ivory, G. G. Miller, J. M. Sowa, L. W. Shacklette, R. R. Chance and R. H. Baughman, *The Journal of Chemical Physics*, 1979, 71, 1506-1507.
137. K. K. Kanazawa, A. F. Diaz, R. H. Geiss, W. D. Gill, J. F. Kwak, J. A. Logan, J. F. Rabolt and G. B. Street, *Journal of the Chemical Society, Chemical Communications*, 1979, DOI: 10.1039/C39790000854, 854-855.
138. R. Hernandez, A. F. Diaz, R. Waltman and J. Bargon, *The Journal of Physical Chemistry*, 1984, 88, 3333-3337.
139. M. R. Bryce, A. Chissel, P. Kathirgamanathan, D. Parker and N. R. M. Smith, *Journal of the Chemical Society, Chemical Communications*, 1987, DOI: 10.1039/C39870000466, 466-467.
140. J.-C. Chiang and A. G. MacDiarmid, *Synthetic Metals*, 1986, 13, 193-205.
141. V. V. Tat'yana and N. E. Oleg, *Russian Chemical Reviews*, 1997, 66, 443.
142. N. Kohut-Svelko, F. Dinant, S. Magana, G. Clisson, J. François, C. Dagron-Lartigau and S. Reynaud, *Polymer International*, 2006, 55, 1184-1190.
143. G. Ćirić-Marjanović, *Synthetic Metals*, 2013, 177, 1-47.
144. A. Pud, N. Ogurtsov, A. Korzhenko and G. Shapoval, *Progress in Polymer Science*, 2003, 28, 1701-1753.
145. A. Bhattacharya and A. De, *Progress in Solid State Chemistry*, 1996, 24, 141-181.
146. M. C. De Jesus, Y. Fu and R. A. Weiss, *Polymer Engineering & Science*, 1997, 37, 1936-1943.
147. R. Gangopadhyay and A. De, *Chemistry of Materials*, 2000, 12, 608-622.
148. M. Akiba and A. S. Hashim, *Progress in Polymer Science*, 1997, 22, 475-521.
149. W. K. Lewis, L. Squires and R. D. Nutting, *Industrial & Engineering Chemistry*, 1937, 29, 1135-1144.
150. B. A. Dogadkin, *Journal of Polymer Science*, 1958, 30, 351-361.

151. J. Tang, L. Kong, J. Zhang, L. Zhan, H. Zhan, Y. Zhou and C. Zhan, *Reactive and Functional Polymers*, 2008, 68, 1408-1413.
152. F. Sun, J. Wang, D. Long, W. Qiao, L. Ling, C. Lv and R. Cai, *Journal of Materials Chemistry A*, 2013, 1, 13283-13289.
153. K. Dong, S. Wang, H. Zhang and J. Wu, *Materials Research Bulletin*, 2013, 48, 2079-2083.
154. Y. Zhang, Y. Zhao, A. Yermukhambetova, Z. Bakenov and P. Chen, *Journal of Materials Chemistry A*, 2013, 1, 295-301.
155. X. Liang, C. Hart, Q. Pang, A. Garsuch, T. Weiss and L. F. Nazar, *Nat Commun*, 2015, 6.
156. Q. Pang, D. Kundu, M. Cuisinier and L. F. Nazar, *Nat Commun*, 2014, 5.
157. X. Tao, J. Wang, Z. Ying, Q. Cai, G. Zheng, Y. Gan, H. Huang, Y. Xia, C. Liang, W. Zhang and Y. Cui, *Nano Letters*, 2014, 14, 5288-5294.
158. S. Evers, T. Yim and L. F. Nazar, *The Journal of Physical Chemistry C*, 2012, 116, 19653-19658.
159. B. Ding, L. Shen, G. Xu, P. Nie and X. Zhang, *Electrochimica Acta*, 2013, 107, 78-84.
160. Z. Wei Seh, W. Li, J. J. Cha, G. Zheng, Y. Yang, M. T. McDowell, P.-C. Hsu and Y. Cui, *Nat Commun*, 2013, 4, 1331.
161. Z. Liang, G. Zheng, W. Li, Z. W. Seh, H. Yao, K. Yan, D. Kong and Y. Cui, *ACS Nano*, 2014, 8, 5249-5256.
162. X. Ji, S. Evers, R. Black and L. F. Nazar, *Nat Commun*, 2011, 2, 325.
163. H. Kim, J. T. Lee, D.-C. Lee, A. Magasinski, W.-i. Cho and G. Yushin, *Advanced Energy Materials*, 2013, 3, 1308-1315.
164. M. Yu, W. Yuan, C. Li, J.-D. Hong and G. Shi, *Journal of Materials Chemistry A*, 2014, 2, 7360-7366.
165. K. T. Lee, R. Black, T. Yim, X. Ji and L. F. Nazar, *Advanced Energy Materials*, 2012, 2, 1490-1496.
166. J. Zheng, J. Tian, D. Wu, M. Gu, W. Xu, C. Wang, F. Gao, M. H. Engelhard, J.-G. Zhang, J. Liu and J. Xiao, *Nano Letters*, 2014, 14, 2345-2352.
167. E. J. Cairns, in *Encyclopedia of Electrochemical Power Sources*, ed. J. Garche, Elsevier, Amsterdam, 2009, vol. 5, pp. 151-154.
168. Y. Liang, Z. Tao and J. Chen, *Advanced Energy Materials*, 2012, 2, 742-769.
169. L. J. Xue, J. X. Li, S. Q. Hu, M. X. Zhang, Y. H. Zhou and C. M. Zhan, *Electrochemistry Communications*, 2003, 5, 903-906.
170. X.-g. Yu, J.-y. Xie, J. Yang, H.-j. Huang, K. Wang and Z.-s. Wen, *Journal of Electroanalytical Chemistry*, 2004, 573, 121-128.
171. X. Yu, J. Xie, Y. Li, H. Huang, C. Lai and K. Wang, *Journal of Power Sources*, 2005, 146, 335-339.
172. Z. Song, H. Zhan and Y. Zhou, *Chemical Communications*, 2009, DOI: 10.1039/B814515F, 448-450.
173. S.-c. Zhang, L. Zhang, W.-k. Wang and W.-j. Xue, *Synthetic Metals*, 2010, 160, 2041-2044.
174. B. Duan, W. Wang, A. Wang, K. Yuan, Z. Yu, H. Zhao, J. Qiu and Y. Yang, *Journal of Materials Chemistry A*, 2013, 1, 13261-13267.
175. W. J. Chung, J. J. Griebel, E. T. Kim, H. Yoon, A. G. Simmonds, H. J. Ji, P. T. Dirlam, R. S. Glass, J. J. Wie, N. A. Nguyen, B. W. Guralnick, J. Park, SomogyiÁrpád, P. Theato, M. E. Mackay, Y.-E. Sung, K. Char and J. Pyun, *Nat Chem*, 2013, 5, 518-524.

176. S. Wei, L. Ma, K. E. Hendrickson, Z. Tu and L. A. Archer, *Journal of the American Chemical Society*, 2015, 137, 12143-12152.
177. Z. Song, Y. Qian, T. Zhang, M. Otani and H. Zhou, *Advanced Science*, 2015, 2, n/a-n/a.
178. J. R. Smith, F. C. Walsh and R. L. Clarke, *Journal of Applied Electrochemistry*, 1998, 28, 1021-1033.
179. D. Zhao, J. Feng, Q. Huo, N. Melosh, G. H. Fredrickson, B. F. Chmelka and G. D. Stucky, *Science*, 1998, 279, 548-552.
180. H.-C. J. Zhou and S. Kitagaw, *Chemical Society Reviews*, 2014, 43, 5415-5418.
181. S. J. Visco, C. C. Mailhe, L. C. De Jonghe and M. B. Armand, *Journal of The Electrochemical Society*, 1989, 136, 661-664.
182. X. Zhang, P. N. Ross, R. Kostecki, F. Kong, S. Sloop, J. B. Kerr, K. Striebel, E. J. Cairns and F. McLarnon, *Journal of The Electrochemical Society*, 2001, 148, A463-A470.
183. B. H. Jeon, J. H. Yeon, K. M. Kim and I. J. Chung, *Journal of Power Sources*, 2002, 109, 89-97.
184. Y.-J. Choi, K.-W. Kim, H.-J. Ahn and J.-H. Ahn, *Journal of Alloys and Compounds*, 2008, 449, 313-316.
185. L. A. Montoro and J. M. Rosolen, *Solid State Ionics*, 2003, 159, 233-240.
186. M. J. Lacey, F. Jeschull, K. Edström and D. Brandell, *Journal of Power Sources*, 2014, 264, 8-14.
187. Z. W. Seh, Q. Zhang, W. Li, G. Zheng, H. Yao and Y. Cui, *Chemical Science*, 2013, 4, 3673-3677.
188. Y. Huang, J. Sun, W. Wang, Y. Wang, Z. Yu, H. Zhang, A. Wang and K. Yuan, *Journal of The Electrochemical Society*, 2008, 155, A764-A767.
189. Q. Wang, W. Wang, Y. Huang, F. Wang, H. Zhang, Z. Yu, A. Wang and K. Yuan, *Journal of The Electrochemical Society*, 2011, 158, A775-A779.
190. H. Schneider, A. Garsuch, A. Panchenko, O. Gronwald, N. Janssen and P. Novák, *Journal of Power Sources*, 2012, 205, 420-425.
191. Z. Zhang, W. Bao, H. Lu, M. Jia, K. Xie, Y. Lai and J. Li, *ECS Electrochemistry Letters*, 2012, 1, A34-A37.
192. M. He, L.-X. Yuan, W.-X. Zhang, X.-L. Hu and Y.-H. Huang, *The Journal of Physical Chemistry C*, 2011, 115, 15703-15709.
193. M. Rao, X. Song, H. Liao and E. J. Cairns, *Electrochimica Acta*, 2012, 65, 228-233.
194. J. Wang, Z. Yao, C. W. Monroe, J. Yang and Y. Nuli, *Advanced Functional Materials*, 2013, 23, 1194-1201.
195. A. Jozwiuk, H. Sommer, J. Janek and T. Brezesinski, *Journal of Power Sources*, 2015, 296, 454-461.
196. M. Rao, X. Song and E. J. Cairns, *Journal of Power Sources*, 2012, 205, 474-478.
197. A. H. Whitehead and M. Schreiber, *Journal of The Electrochemical Society*, 2005, 152, A2105-A2113.
198. S.-H. Chung and A. Manthiram, *Journal of Materials Chemistry A*, 2013, 1, 9590-9596.
199. X.-B. Cheng, H.-J. Peng, J.-Q. Huang, L. Zhu, S.-H. Yang, Y. Liu, H.-W. Zhang, W. Zhu, F. Wei and Q. Zhang, *Journal of Power Sources*, 2014, 261, 264-270.
200. G. Zhou, L. Li, C. Ma, S. Wang, Y. Shi, N. Koratkar, W. Ren, F. Li and H.-M. Cheng, *Nano Energy*, 2015, 11, 356-365.
201. Y.-S. Su and A. Manthiram, *Nat Commun*, 2012, 3, 1166.
202. G. Ma, Z. Wen, J. Jin, M. Wu, X. Wu and J. Zhang, *Journal of Power Sources*, 2014, 267,

542-546.
203. X. Wang, Z. Wang and L. Chen, *Journal of Power Sources*, 2013, 242, 65-69.
204. C. Zu, Y.-S. Su, Y. Fu and A. Manthiram, *Physical Chemistry Chemical Physics*, 2013, 15, 2291-2297.
205. T.-G. Jeong, Y. H. Moon, H.-H. Chun, H. S. Kim, B. W. Cho and Y.-T. Kim, *Chemical Communications*, 2013, 49, 11107-11109.
206. G. Zhou, S. Pei, L. Li, D.-W. Wang, S. Wang, K. Huang, L.-C. Yin, F. Li and H.-M. Cheng, *Advanced Materials*, 2014, 26, 625-631.
207. S.-H. Chung and A. Manthiram, *Chemical Communications*, 2014, 50, 4184-4187.
208. H. Yao, K. Yan, W. Li, G. Zheng, D. Kong, Z. W. Seh, V. K. Narasimhan, Z. Liang and Y. Cui, *Energy & Environmental Science*, 2014, 7, 3381-3390.
209. K. Zhang, F. Qin, J. Fang, Q. Li, M. Jia, Y. Lai, Z. Zhang and J. Li, *J Solid State Electrochem*, 2014, 18, 1025-1029.
210. J.-Q. Huang, B. Zhang, Z.-L. Xu, S. Abouali, M. Akbari Garakani, J. Huang and J.-K. Kim, *Journal of Power Sources*, 2015, 285, 43-50.
211. J. Song, Z. Yu, T. Xu, S. Chenm H. Sohn, M. Regula and D. Wang, *Journal of Materials Chemistry A*, 2014, 2, 8623.
212. L. Miao, W. Wang, A. Wang, K. Yuan and Y. Yang, *Journal of Materials Chemistry A*, 2013, 1, 11659.

Figures

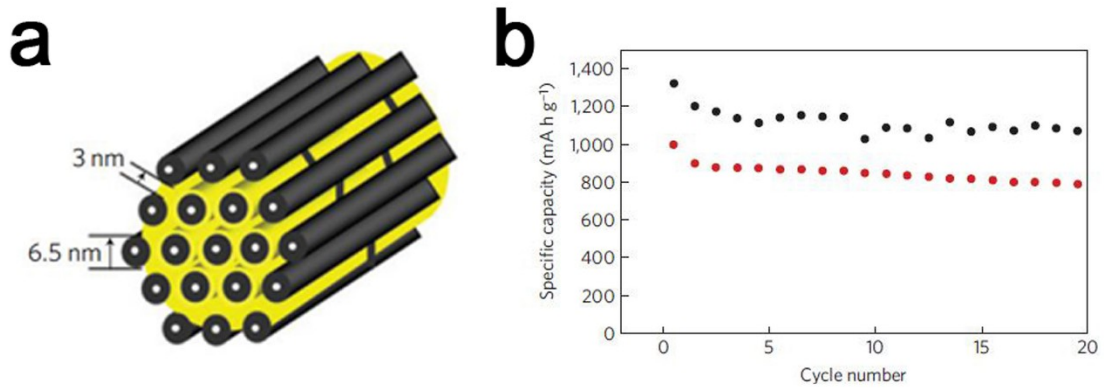

Figure 1. (a) A schematic diagram of sulfur (yellow) confined within the interconnected pore structure of mesoporous carbon (CMK-3) formed from carbon tubes that are held together by carbon nanofibers. (b) Cycling stability comparison of CMK-3/S-PEG (upper points, in black) versus CMK-3/S (lower points, in red) at 168 mA/g at room temperature.[45]

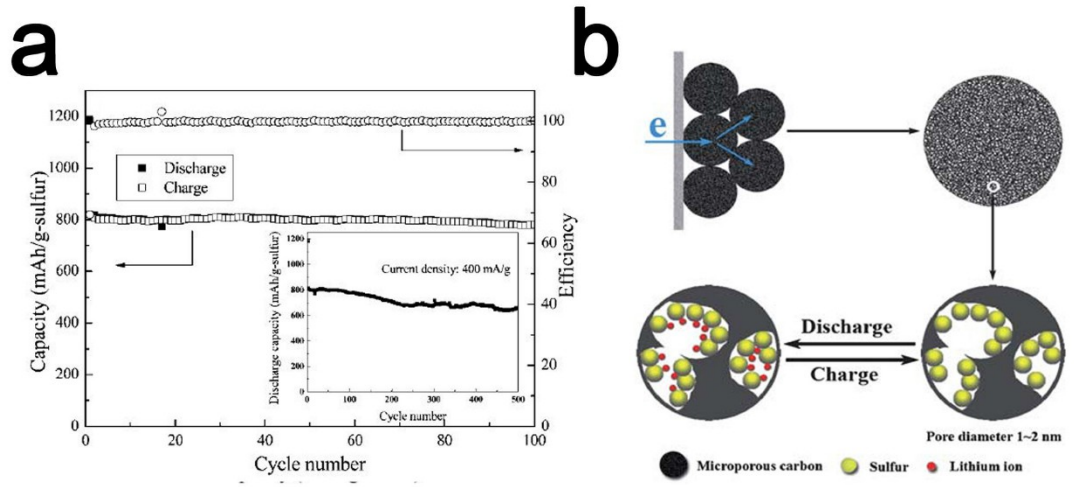

Figure 2. (a) The cycling performance of a sulfur–carbon composite with 42 wt% sulfur the constant specific current of 400 mA/g (inset: The long cycle life of the composite at the specific current of 400 mA/g). (b) A scheme of the constrained electrochemical reaction process inside the micropores of the sulfur–carbon sphere composite cathode.[46]

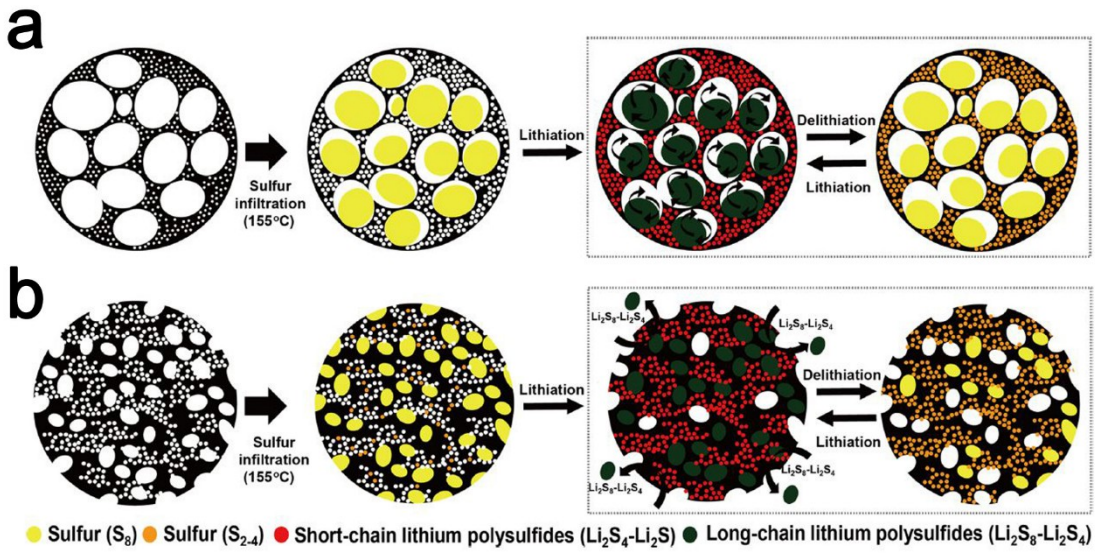

Figure 3 Schematic illustration of the electrode structures and their electrochemical processes. (a) Hierarchical porous carbon particles have micropores in the outer shell, surrounding the inner meso- and macropores. The dissolution of the soluble long-chain lithium polysulfides in the inner macro- and mesopores is suppressed by the outer micropores serving as a barricade. (b) Conventional activated carbon (AC1600) containing micropores and mesopores in a random geometry. The long-chain lithium polysulfides are liable to dissolution through the open pore ends.[54]

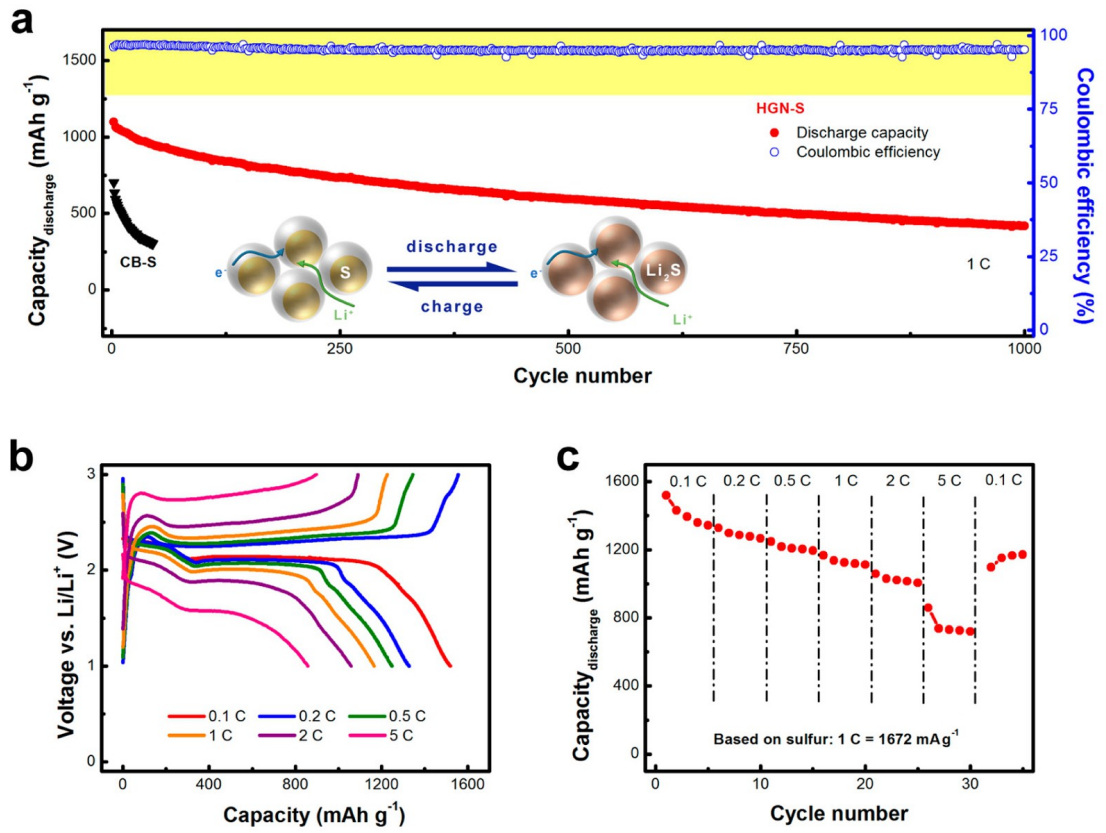

Figure 4 Electrochemical performance of HGN-S. (a) Cycling performance at a rate of 1 C and schematic illustration of HGN-S during discharge and charge (inset), (b) galvanostatic charge-discharge profiles at different rates, and (c) rate performance.[71]

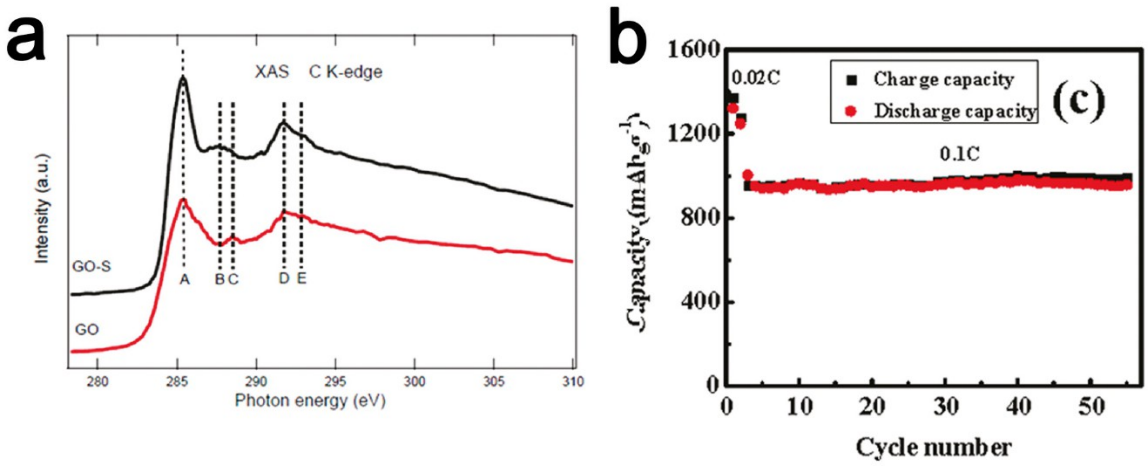

Figure 5 (a) C K-edge XAS spectra of GO and GO-S nanocomposites after heat treatment in Ar at 155 ^{o}C for 12 h. (b) cycling performance of GO-sulfur nano-composite cathode at a constant rate of 0.1C after initial activation processes at 0.02C for two cycles.[67]

Figure 6 Long-term cycling test results of a Li/S cell with a CTAB-modified sulfur/GO nano-composite cathode. (inset: schematic illustration of CTAB-modified sulfur/GO nano-composite.[88]

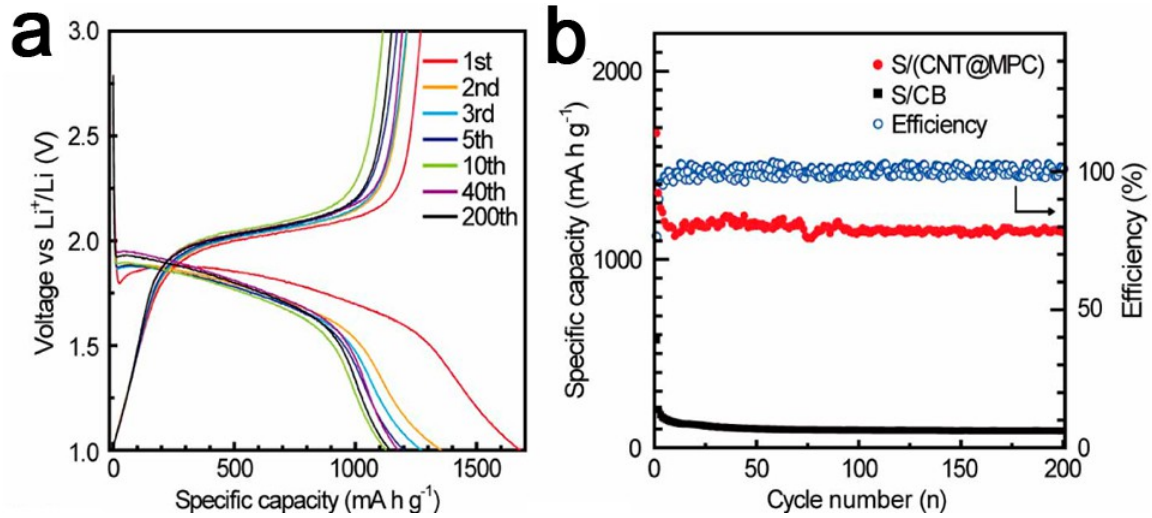

Figure 7 Electrochemical properties in carbonate-based electrolyte. (a) Voltage profiles of S/(CNT@MPC) at 0.1 C. (b) Cycling performance of S/(CNT@MPC) and S/CB at 0.1 C (blue circles show the Coulombic efficiency of S/(CNT@MPC)).[102]

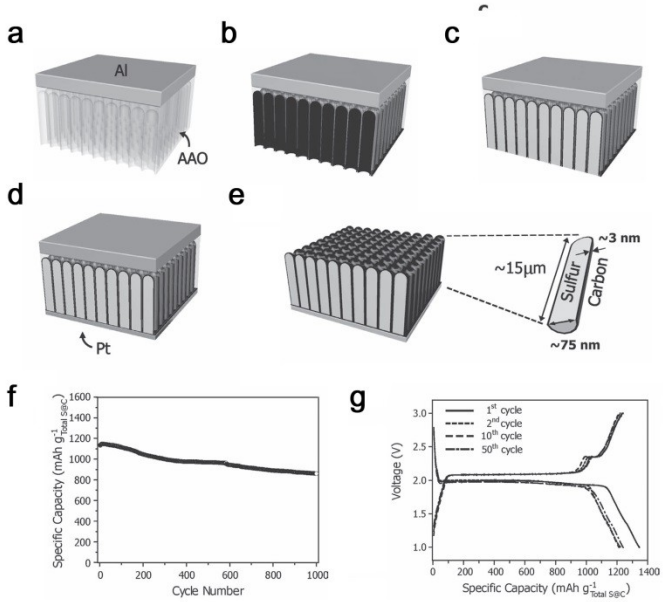

Figure 8 Schematic illustration of the fabrication procedure of the S@C NW electrode. (a) Preparation of porous alumina template by a two-step anodization process. (b) Carbon layer deposition by a CVD process to form an array of CNTs. (c) Sulfur infiltration utilizing capillary force through a heat-treatment at 155 °C. (d) Pt deposition on the opposite side and a heat-treatment at 400 °C. (e) The final electrode structure after removal of the membrane by a wet etching step, alongside a schematic of each S@C NW with the dimensions of the key components denoted. Electrochemical characterization of the S@C NW electrode. (f) Capacity retention at the discharge rate of 5.0 and the charge rate of 2.0 C for 1000 cycles. (g) Galvanostatic profiles of the S@C electrode at different cycle numbers when measured at 0.5 C for both charge and discharge (1 C = 1675 mA/g).[107]

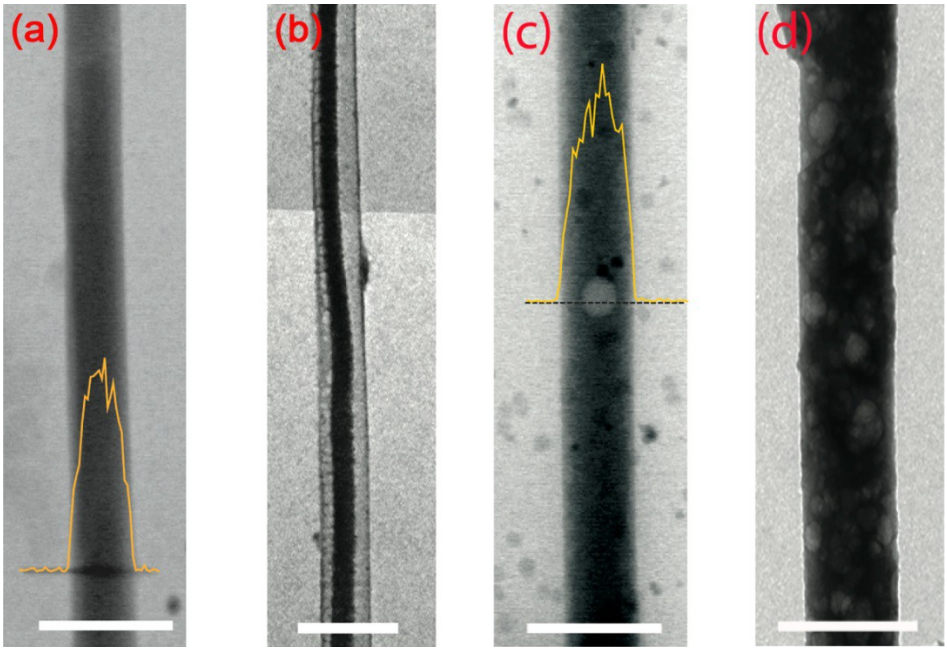

Figure 9 *Ex-situ* study of hollow carbon nanofiber encapsulated sulfur cathode. (a) TEM image of the sulfur cathode

before discharge. The yellow line represents the EDS counts of the sulfur signal along the dark line. (b) TEM image of the sulfur cathode after full discharge to 1.7 V. (c) TEM image of the sulfur cathode after functionalization with polymer and infusion of sulfur. The yellow line represents the EDS count of the sulfur signal along the dashed line. (d) TEM image of the sulfur cathode after full discharge. The scale bars are 500 nm.[108]

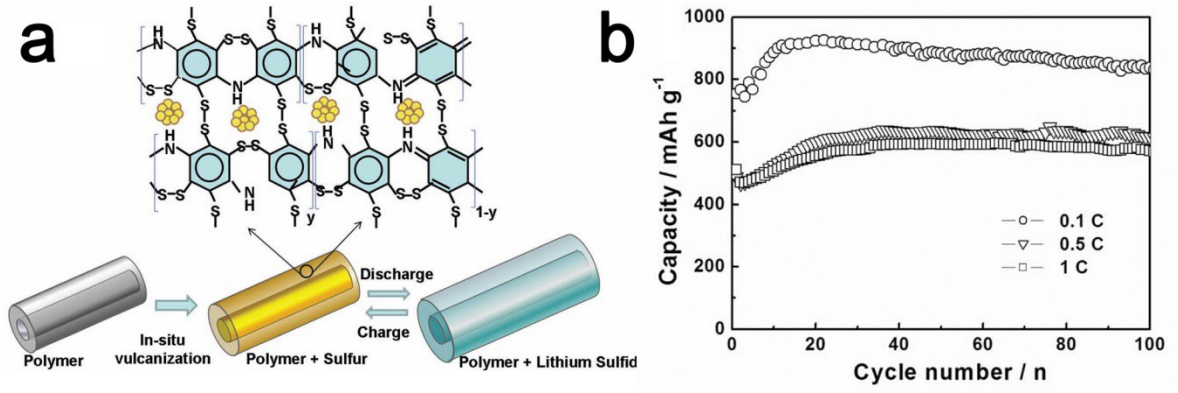

Figure 10 (a) Schematic illustration of the construction and discharge/charge process of the SPANI-NT/S composite. (b) Discharge capacity vs. cycle number of the SPANI-NT/S composite electrode at different rates as labeled.[116]

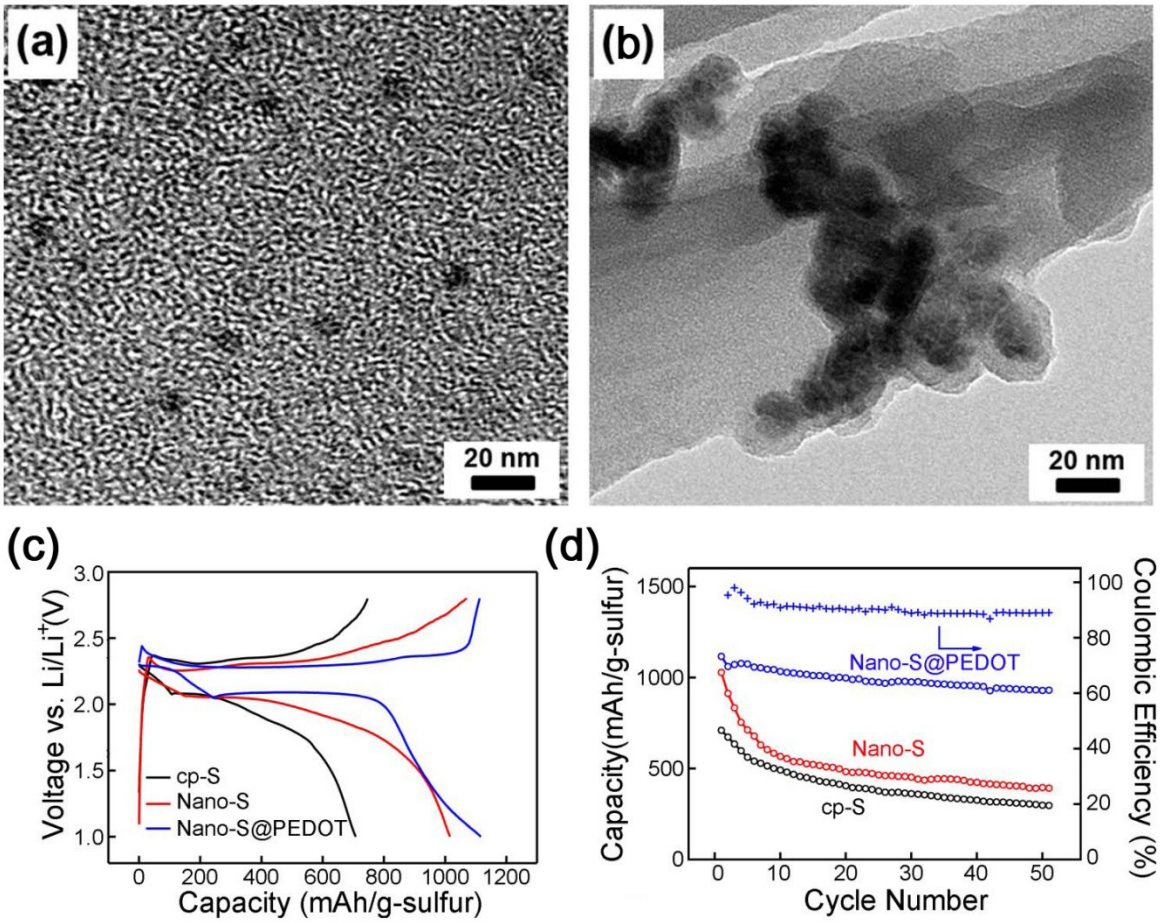

Figure 11 TEM images of (a) pure S nanoparticles and (b) S/PEDOT core/shell nanoparticles. (c) Initial discharge/charge curves of Nano-S@PEDOT (blue), Nano-S (red), and CP-S (black) cathodes at a specific current of 400 mA/g (0.25 C) (d) Discharge capacity and Coulombic efficiency cycling stability for Nano-S@PEDOT (blue), Nano-S (red), and CP-S (black) cathodes at a specific current of 400 mA/g.[132]

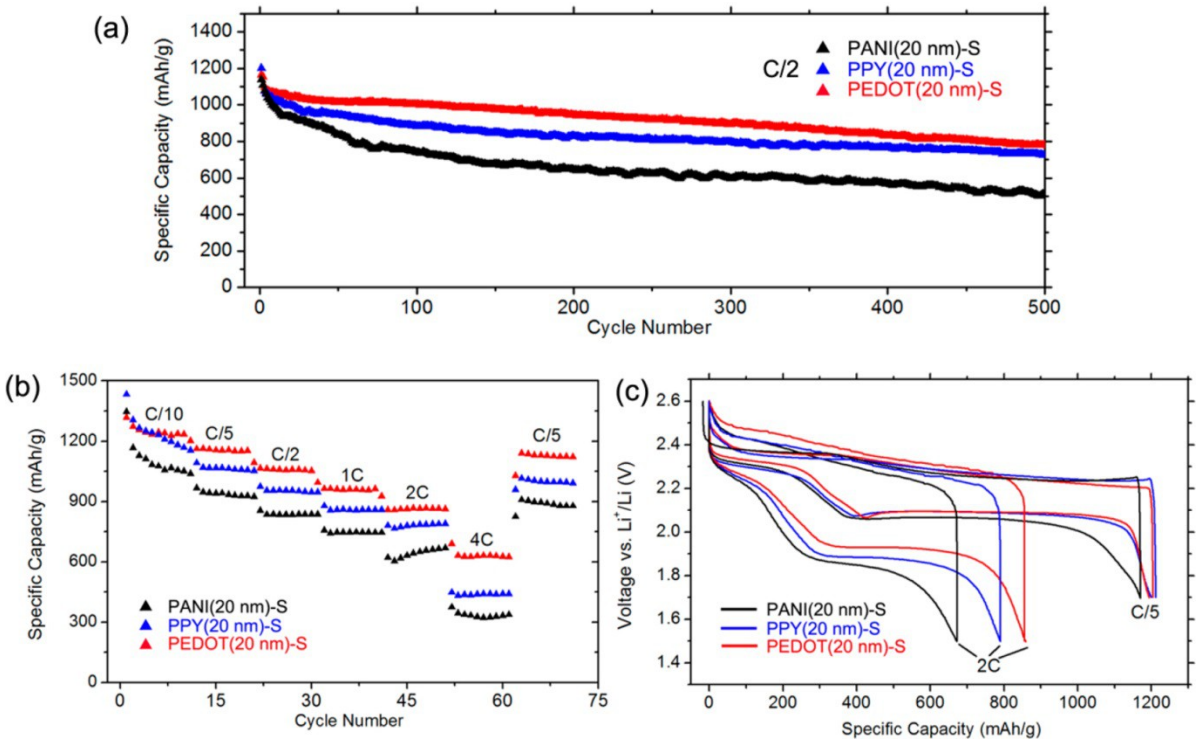

Figure 12 (a) Cycling performance of the cells made from hollow sulfur nanospheres with PANi, PPY, and PEDOT coatings of ∼20 nm at C/2 rate for 500 cycles. (b) Rate capability of the cells discharged at various rates from C/10 to 4C. (c) Typical discharge−charge voltage profiles of the cells at 0.2 C and 2.0 C (1 C = 1673 mA/g).[121]

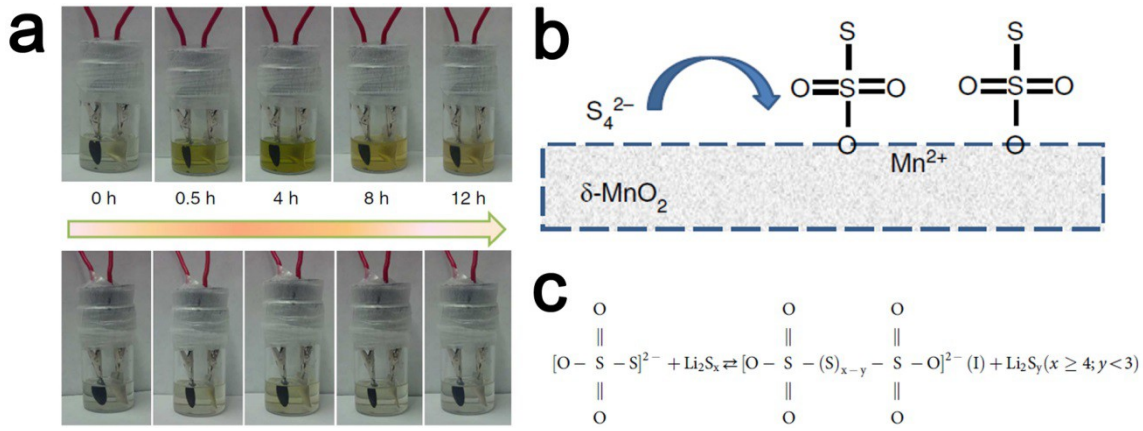

Figure 13 (a) Visual confirmation of polysulfide entrapment at specific discharge depths. (upper: S/KB, lower: S/MnO_2 cells.) (b) Schematic showing the oxidation of initially formed polysulfide by d-MnO_2 to form thiosulfate on the surface, concomitant with the reduction of Mn^{4+} to Mn^{2+}. (c) Reaction chemistry of thiosulfate on the surface of MnO_2 to anchor soluble long-chain polysulfides and its conversion to insoluble lower polysulfide that is Li_2S_2 or Li_2S.[155]

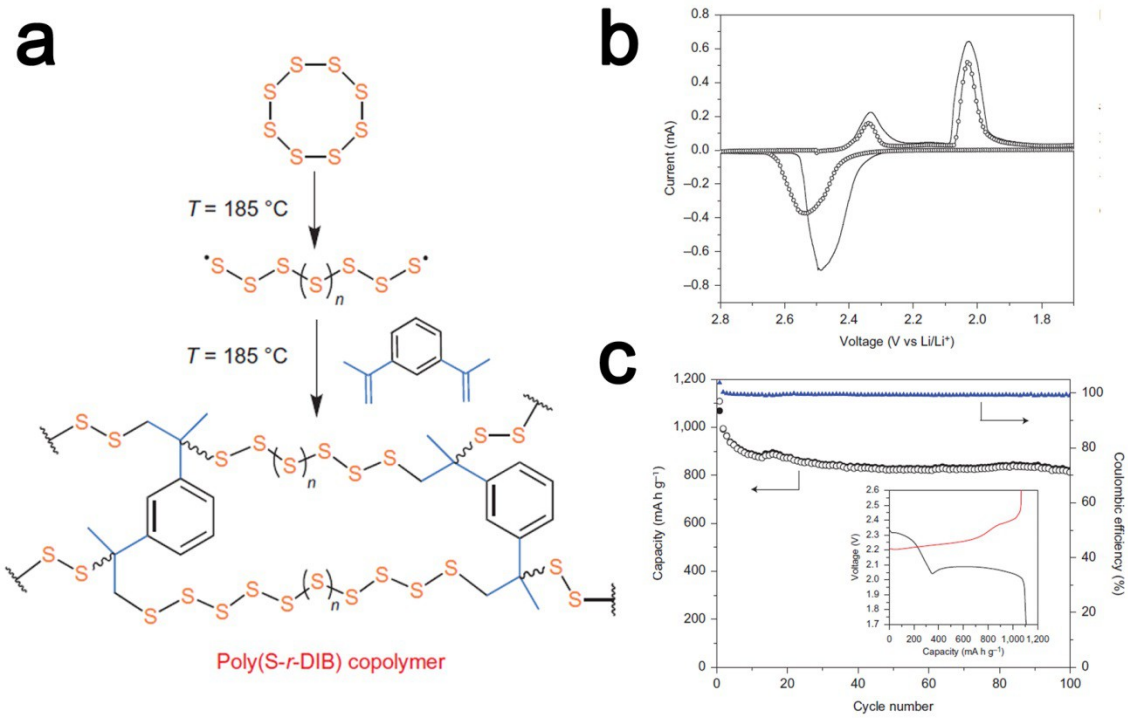

Figure 14 (a) Synthetic scheme for the copolymerization of S_8 with DIB to form chemically stable sulfur copolymers. Electrochemical performance of the poly(S-r-DIB) cathode. (b) CV of the S_8 (solid black line) and the poly(S-r-DIB) cathodes at a scan rate of 20 μV/s. (c) Cell cycling data for the poly(S-r-DIB) cathode showing the discharge capacity (open circles), charge capacity (filled circles) and Coulombic efficiency (blue triangles) with the inset showing a typical charge/discharge profile.[175]

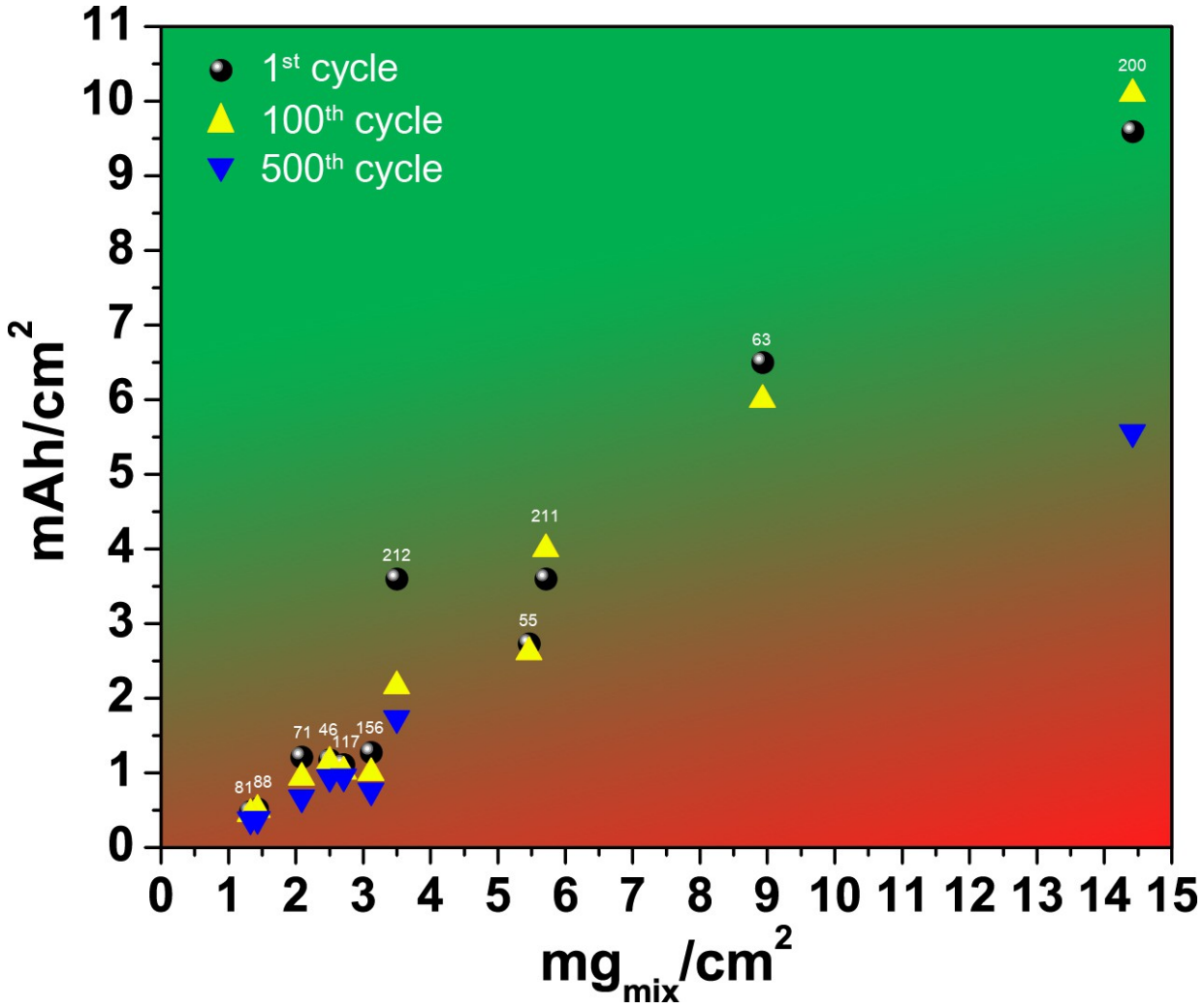

Figure 15 Estimated cell capacity/cm^2 plot as a function of the mixture weight/cm^2 of the cathode. The capacity/cm^2 of the cathodes for the first cycle (circle), 100th cycle (triangle) and 500th cycle (inverted triangle) are marked. Each number indicates the reference number of the work cited at the end of this chapter.

Table

Compound	Gram per equivalent (g/eq)	Chemical structure	Theoretical specific capacity (mAh/g)
2,5-Dimercapto-1,3,4-thiadiazole (DMcT)	74	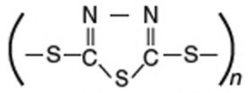	362
Dimethyl ethylenediamine	75	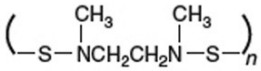	357
2-Mercapto-5-methyl-1,3,4-thiadiazole (McMT)	131	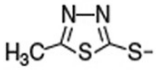	205
Anthra[1',9',8'-b,c,d,e][4',10',5'-b',c',d',e'] bis-[1,6,6a(6a-S^{IV}) trithia]pentalene (ABTH)	60.7	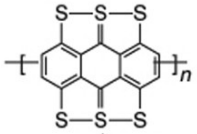	442
Poly(5,8-dihydro-1H,4H-2,3,6,7-tetrathiaanthracene)(PDTTA)	64	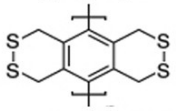	419
Polydithiodianiline (poly(DTDA))	121	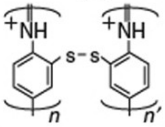	222

Table 1. Some organosulfur compounds investigated as positive electrodes.